



**Samueli**  
Civil & Environmental Engineering



**Jet Propulsion Laboratory**  
California Institute of Technology

## **Evaluating the Application of Remote Sensing and Lab-Based Methods to Analyze Water Quality in Los Angeles Coastal Waters**

UCLA Environmental Science Practicum Program 2021-2022

Client: Christine Lee, Ph.D., of NASA's Jet Propulsion Laboratory

Faculty Advisor: Jennifer Jay, Ph.D.

Graduate Advisor: Yuwei Kong

Secondary Graduate Advisor: Karina Jimenez

Team Members: Sophia Winter, Jasmine Summers-Evans, Cade Mills, Max Menczer,  
Albert Cao, Kierstin Blatzheim, Rachel Han, and Savannah McCarthy



## TABLE OF CONTENTS

1. Abstract.....	1
2. Background.....	2
2.1 - What are antibiotic-resistant bacteria and antibiotic-resistant genes?	
2.2 - Antibiotic-resistant bacteria and antibiotic-resistant genes in the environment	
2.3 - Antibiotic-resistant genes and their threat to public health	
2.4 - Fecal indicator bacteria and ESBL - <i>E. coli</i>	
2.5 - Key indicators of water quality	
2.6 - The relationship between total suspended solids, turbidity, and bacteria levels	
2.7 - <i>In situ</i> sampling and methods for monitoring microbial water quality	
2.8 - IDEXX method and antibiotic-resistant bacteria	
2.9 - Remote sensing as a tool for digital water quality monitoring	
3. Research Questions.....	14
4. Methods: Water Quality.....	15
4.1 - On-site measurements	
4.2 - In-lab measurements	
5. Methods: Fecal Indicator Bacteria.....	18
5.1 - IDEXX method	
5.2 - Filter-plating method	
6. Methods: Remote Sensing and Data Analysis.....	21
6.1 - Remote sensing data acquisition	
6.2 - Regression models for turbidity	
6.3 - Comparison between IDEXX and filter-plating method	
7. Results.....	23
7.1 - Data collection and testing for correlations	
7.1 - Satellite-derived turbidity	
7.3 - Simple linear regression for turbidity	
7.4 - Multiple linear regression and ridge Regression for turbidity	
7.5 - Random forest regression for turbidity	
7.6 - Additional water quality metrics	
7.7 - IDEXX vs. filter-plating method	

7.8 - Fecal indicator bacteria vs. turbidity	
7.9 - Spatial distribution of <i>E. coli</i>	
8. Discussion.....	34
8.1 - Simple linear regression for turbidity	
8.2 - Multiple linear regression, ridge regression, and random forest for turbidity	
8.3 - Future research with Landsat	
8.4 - IDEXX vs. filter-plating method	
8.5 - Bacterial growth mode: planktonic vs. biofilm	
8.6 - Fecal indicator bacteria vs. turbidity	
8.7 - Spatial distribution of <i>E. coli</i>	
8.8 - Seasonal effects	
8.9 - Potential sources of error	
9. Conclusion.....	41
10. Acknowledgements .....	41
11. References.....	43
12. Appendix.....	55

## 1. ABSTRACT

Two common metrics used to measure water quality are fecal indicator bacteria (FIB) content and turbidity. FIB content measures a water's bacterial contamination. Certain FIB are pathogenic, and some are able to develop resistance to antibiotics designed to inhibit them. Turbidity measures the murkiness of water due to suspended solids, which can be an indicator of higher bacteria content. Both metrics can be time- and labor-intensive to measure in a lab. To reduce the risk of pathogen exposure in recreational waters, it is critical to make water quality monitoring more accessible. Through the use of two efficient techniques, remote sensing and the IDEXX Quanti-Tray 2000 method, turbidity was modeled as a proxy for FIB and antibiotic-resistant bacteria. Water samples were obtained from eight coastal sites: Venice Beach, Santa Monica Beach, Pacific Palisades Beach, Topanga Beach, three beach sites around the Malibu Lagoon, and Zuma Beach. Both filter-plating and the IDEXX method were used to detect the presence of FIB and antibiotic-resistant bacteria. Turbidity values were derived from satellite observations and compared to on-site turbidity readings, bacteria content, and other key water quality metrics. There was a low correlation between satellite-derived turbidity and turbidity measured on-site. The IDEXX method had a low correlation with filter-plating for detecting antibiotic-resistant *E. coli*, but a high correlation for detecting total *E. coli* levels. Overall, bacteria levels were highest at Santa Monica, and antibiotic-resistant bacteria levels were highest around the Malibu Lagoon. More research is required on the ability for satellite-derived turbidity and the IDEXX method to serve as proxies for assessing contamination of FIB and antibiotic-resistant bacteria in coastal waters.

## **2. BACKGROUND**

### ***2.1 - What are antibiotic-resistant bacteria and antibiotic-resistant genes?***

Antibiotics encompass a wide range of chemical compounds that can be produced naturally, semi-synthetically, and synthetically (Manyi-Loh et al., 2018). In humans and animals, antibiotics are used to fight bacterial infections by killing bacteria or stopping bacterial growth (CDC, 2020). However, bacteria are constantly evolving and passing on new genetic material that makes them increasingly resistant to the antibiotics designed to inhibit them. In 1942, the first antibiotic-resistant bacteria (ARB), *Staphylococcus aureus*, was discovered. The race between effective antibiotics and bacterial resistance has not stopped since (CDC, 2020).

The creation of and selection for ARB is caused by the consistent, frequent, and, in some cases, improper use of antibiotics (Le et al., 2018). Every time an antibiotic is used, there is an opportunity for bacteria to become resistant (Wu et al., 2019). When there is exposure to an antibiotic, microbial communities can share resistant genes across genera to positively select for new resistant strains, even at heightened metabolic costs (Griffin et al., 2020). Bacteria can become resistant to antibiotics by either intracellular mutation or by acquiring mobilized antibiotic-resistant genes (ARGs) from other bacteria (Wu et al., 2019). ARGs are found in plasmids, which serve as mobile carriers for genetic information. Horizontal transfer of plasmids allows bacteria to adapt to antibiotics and acquire these ARGs at an alarmingly quick rate in the human body (Stalder et al., 2019). This process can alter the human microbiome and cause health disturbances.

### ***2.2 - Antibiotic-resistant bacteria and antibiotic-resistant genes in the environment***

Unlike other chemical and organic pollutants that can degrade or decrease in concentration over time, microbial contaminants and ARGs can remain alive and multiply in environments for long periods of time (Berendonk et al., 2015). Their entry rate into the environment is higher than their elimination rate, making them “persistent” or “pseudo-persistent” substances (Coman, 2016). One study demonstrated that low concentrations of antibiotics in the environment can bring about random and spontaneous mutagenesis, making the environment a reservoir for antibiotics, ARB, and their resistance genes (Cogliani et al., 2011). Therefore, antibiotic residues and their associated ARB and ARGs are considered

environmental pollutants with the power to affect whole environmental microbiomes (Xi et al., 2009; CDC, 2021).

Wastewater treatment plants (WWTPs), medical waste streams, and animal agriculture have been identified as key sources for antibiotics, ARB, and ARGs to enter the environment (Kim et al., 2021). Waste produced by humans and livestock who have been treated with an antibiotic contains residual, unmetabolized amounts of the antibiotic. This waste can be expelled into freshwater and marine ecosystems through either direct runoff into a waterway or WWTP effluent (Nnadozie et al., 2019). Since WWTPs are the bridge between human waste and the environment, many studies have been conducted on the efficacy of WWTP technologies to remove and screen for ARB and ARGs. Currently, the complete removal of ARB and ARGs from WWTPs is not possible (Xu et al., 2016; Amarasiri et al., 2019). WWTP operations are only capable of removing about 53-78% of antibiotics globally (Wang et al., 2020). In agricultural settings, the saturation of livestock with antibiotics in the U.S. and other countries has led to an increase in antibiotic resistance in the soil and waste products from agricultural sites (Hollis and Ahmed, 2013). There is a direct link between antibiotic use in livestock agriculture and antibiotic resistance in the environment (Economou and Gousia, 2014). Up to 75% of the antibiotics administered to feedlot livestock can be excreted in animal waste, so it is likely that a significant amount of antibiotics enter adjacent water systems (Roe & Pillai, 2003). Once disseminated into the environment, aquatic ecosystems such as rivers, oceans, and estuaries serve as primary transmission routes of antibiotic resistance (Kim et al., 2021). In seawater, 90% or more of bacteria strains are resistant to at least one antibiotic, and 20% are resistant to two or more antibiotics (Baquero et al., 2008).

The movement of ARB in natural environments is directly affected by weather events. ARB that are regularly detected in water bodies can be measured at significantly higher concentrations after a stormwater event (Zhang et al., 2016; Rugh, 2021). It can often be difficult to show a direct link between increased concentrations of ARB pollution from wet-weather conditions and human health problems. However, a Practicum Project led by Dr. Jennifer Jay in 2019 demonstrated that a pathogenic ARB was colonizing surfers at a higher rate during wet-weather events (Rugh, 2021). This study tracked methicillin-resistant *Staphylococcus aureus* (MRSA) colonization in surfers because they frequently expose themselves to coastal waters year-round, including during the wet season. People that surfed during wet weather were over

three times more likely to be colonized by MRSA compared to dry-weather surfers and over six times more likely to be colonized by MRSA compared to non-surfers. The continuous sampling of these surfers enabled the study to draw a direct link between MRSA colonizations and degraded coastal water quality.

### ***2.3 - Antibiotic-resistant genes and their threat to public health***

It is important to note that antibiotic resistance is an ancient process that predates clinical antibiotic usage (Watts et al., 2017). Antibiotics occur naturally and are found in many types of aquatic and terrestrial environments. However, large-scale, often unregulated, anthropogenic use of antibiotics can undermine the objective of their creation- to save lives and protect against disease. Antibiotic-resistant infections result in longer hospitalization times and require intake of stronger and more expensive medicines, resulting in higher medical costs and patient complications. The 2 million annual cases of antibiotic-resistant infections in the U.S. result in approximately 23,000 deaths each year (Griffin et al., 2020). Because there are no geographic boundaries to the spread of antibiotic resistance, this creates a truly global problem. Without considerable mitigation, it is projected that deaths associated with ARB around the world may surpass deaths due to cancer by 2050 (Griffin et al., 2020). In response to concerns around antibiotic resistance, the World Health Organization now demands that each country develops a national action plan relative to their financial resources and the extent of the concern within their country (World Health Assembly, 2016). In conjunction with regulatory improvements, continued research on environmental antibiotic resistance is essential for best understanding how to protect public health.

### ***2.4 - Fecal Indicator Bacteria and ESBL - E. coli***

When conducting surveillance of antibiotic resistance in the environment, fecal indicator bacteria (FIB) are often focused on because of their pathogenic potential and ability to acquire resistance easily (Reinthal et al., 2003; Collignon, 2009). FIB are bacteria that live in the gut of warm-blooded animals and are introduced into the environment through fecal matter (NOAA GLERL, n.d.). While FIB are generally harmless, they indicate the possible presence of other pathogenic bacteria, viruses, and protozoans found in fecal matter and correlate with the occurrence of certain waterborne diseases (US EPA, n.d.c). Since testing for the presence of

many different pathogens is resource-intensive, water systems are typically tested for a few subgroups of bacteria instead. The most commonly tested FIB include total coliforms, fecal coliforms, *Escherichia coli* (*E. coli*), fecal streptococci, and enterococci.

Total coliforms are a widespread group of bacteria that can occur in human feces, but also in other places outside the human body. For drinking water, total coliforms are still a standard indicator test because their presence implies contamination of a water supply by an outside source. Fecal coliforms are a subset of total coliform bacteria, which are more fecal-specific in origin. For recreational waters, this group was used as the primary bacteria indicator until relatively recently when the EPA began recommending *E. coli* and enterococci as preferred indicators of health risk. *E. coli* is a species of fecal coliform bacteria that is considered the best indicator bacteria to use for recreational water quality monitoring because of its specificity, ease of detection, and how well studied it has been (McLain et al., 2016; Wuijts et al., 2017; Vikesland et al., 2017). In the past, ratios of fecal streptococci to fecal coliforms were monitored to determine whether contamination was of human or nonhuman origin. This is no longer recommended as a reliable bacterial source tracking test though. Lastly, enterococci are a subgroup of fecal streptococci and are distinguished by their ability to survive in saltwater conditions. Because of this, the EPA now recommends enterococci as the primary indicator of health risk in salt water used for recreation.

Since these bacteria commonly reside in the intestines of warm-blooded animals, they are subjected to frequent exposure to antibiotics consumed by their host and high selection pressure (Khardori, 2012). As an example, *E. coli* can be used to measure antibiotic resistance by looking at extended-spectrum  $\beta$ -lactamase producing *E. coli* (ESBL-*E. coli*). ESBLs are plasmid-mediated enzymes produced by *E. coli* that inhibit  $\beta$ -lactam antibiotics (e.g. penicillins, cephalosporins, carbapenems) (Fuentes et al., 2019; Shanthi & Sekar, 2010). These enzymes also show co-resistance to many other classes of antibiotics. Infections caused by ESBLs can range from UTIs to life-threatening sepsis (Rawat & Nair, 2010). With the spread of antibiotic resistance accelerating, monitoring bacteria like ESBL-*E. coli* is critical.

### ***2.5 - Key indicators of water quality***

In addition to monitoring bacteria content and antibiotic resistance in water systems, water quality also encompasses a large variety of chemical, physical, and biological properties.

For aquatic ecosystems, several widely accepted indicators are used by most monitoring agencies. Key indicators can include (but are not limited to) temperature, pH, conductivity, dissolved oxygen content, turbidity, total suspended solids (TSS), light absorbance, and nutrient levels. Table 1 briefly describes these parameters.

**Table 1.** Summary of key parameters monitored for water quality.

Parameter	Description
pH	Measure of free hydrogen and hydroxyl ions in the water. Determines the solubility of chemical constituents. Controls availability of chemicals used as nutrients by organisms (USGS Water Science School, 2019).
Conductivity	Measure of the water's ability to carry an electrical current. Higher conductivity is created by presence of salts and other inorganic compounds (US EPA, 2013a).
Dissolved Oxygen	Measure of how much oxygen is available for use by aquatic life. Directly linked to the presence of inorganic compounds and temperature (USGS Water Science School, 2018a).
Turbidity	Measure of water clarity derived from the reflectivity of light that is scattered by material in the water (Hannouche, 2011). Higher turbidity can be caused by clay, silt, inorganic and organic matter, algae, plankton, and other microscopic organisms (USGS Water Science School, 2018b).
Total Suspended Solids	Measure of particles suspended in water that will not pass through a 1.5-micron filter. Suspended solids include silt, clay, plankton, algae, fine organic debris, and other particulate matter (US EPA, n.d.b).
Light Absorbance	Measure of amount and wavelength of light that can pass through water. Can be measured remotely via satellite or using a spectrometer. Chemical compounds and organic materials can absorb different wavelengths of light (Wormell & Rodger, 2013).
Nutrients	Measure of various nutrients present in water, which often include nitrogen and phosphorus species (e.g. ammonia, nitrate, and phosphate). Too much of any of these compounds can lead to eutrophication and overproliferation of algae, which depletes dissolved oxygen levels (Greenberg et al., 1992).

## ***2.6 - The relationship between total suspended solids, turbidity, and bacteria levels***

TSS is typically measured as a concentration in mg/L. Turbidity, on the other hand, is measured in both nephelometric turbidity units (NTU) and Formazin Attenuation Units (FAU). These different units make it challenging to convert TSS measurements into turbidity and vice versa. Instead, researchers have been looking for trends and relationships between the two variables. In recent years, there have been many studies analyzing the relationship between TSS and turbidity, and investigating if one could be used to estimate the other and reduce data collection demands.

While TSS and turbidity both relate to the amount of suspended solids in water, the uses for each parameter vary. The benefit of TSS analysis is that it is representative of environmental concerns. High TSS conditions can block the gills of fish, carry bacteria, and have other detrimental effects on water quality. Federal agencies place limits on TSS concentrations in bodies of water, especially close to dredging and waste disposal locations (Thackston, 2000). TSS measurements take several hours though and can only be conducted within a lab. This is not ideal during wet weather events when water conditions change rapidly, making TSS sampling less useful. Turbidity measurements can be taken quickly and frequently, providing real-time values that better reflect current water conditions. Turbidity can also be derived from remotely-sensed observations, whereas TSS cannot. However, turbidity does not have a conclusive correlation to environmental impact concerns (Thackston, 2000).

There have been several studies that suggest a positive relationship between TSS concentration and total coliform levels (Aram, 2021; Irvine et al., 2002; Murray et al., 2001). Irvine et al. described this relationship in the equation  $\text{Log}(\text{Fecal Coliforms}) = A + B(\text{Log}(\text{TSS}))$ , where A and B are empirical constants that vary with space and time (Irvine et al., 2002). Suspended solids may be helpful to bacteria's survival in the form of shelter or nutrients, but the exact mechanism behind the correlation between TSS and fecal bacteria concentrations remains unknown (Aram, 2021).

At WWTPs, turbidity is one of the most widely tested parameters that helps determine the effectiveness of wastewater treatment (Operators Unlimited, 2021). Turbidity-causing materials (TCMs) vary widely depending on water type and location (Diamant, 2013). The causes of turbidity and composition of TCMs are dependent on the water source and/or the treatment system. TCMs can be vehicles for bacteria to proliferate during wastewater treatment,

so it is essential to reduce turbidity for effective disinfection (Cleveland Water Department, 2019). In potable water, turbidity is not always representative of harmful conditions, but is aesthetically unappealing and can be indicative of a health risk depending on the specific TCMs present (Diamant, 2013). The Centers for Disease Control and Prevention requires all treated water to be below 0.3 NTU turbidity to protect against bacteria like *Cryptosporidium* entering surface water sources (CDC, 2019). *Cryptosporidium* is a microscopic parasite that causes diarrheal disease if ingested.

There has been little research into the direct link between turbidity and bacteria concentration or public health risk in coastal waters. Existing literature reveals relationships between turbidity and bacteria just above the statistically significant threshold (Aram, 2021). However, these relationships are not conclusive, with some studies suggesting positive relationships and others suggesting negative relationships (Aram, 2021; Mallin et al., 2009). This inconsistency seems to suggest that relationships between turbidity and bacteria in ocean water may vary spatially or temporally.

## ***2.7 - In situ sampling and methods for monitoring microbial water quality***

Routine water quality monitoring is necessary for the protection of ecosystems and public health, but methods can be limited by long turnaround times (24+ hours), unavailability of trained staff, lack of equipped labs, and insufficient funding (Kinzelman et al., 2005). Currently, direct field sampling is the primary monitoring method for the water quality parameters discussed above (Table 1). Samples are generally collected and brought back to a lab for analysis, or when possible, measurement devices can be installed in the field for long-term, continuous data collection.

For monitoring microbial water quality specifically, there are several main lab methods. Multiple-tube fermentation, membrane filtration/filter-plating, and defined substrate technologies are all methods used to quantify FIB in water samples (Budnick et al., 1996; Rompré et al., 2002). All three methods rely on temperature, substrate, and selective growth inhibitors to select for FIB (Fricker & Fricker, 1996; Sercu et al., 2011). Historically, culture-based techniques where target bacteria are isolated on selective media and assessed for growth have been the gold standard. However, culture-based methods can be costly and time-consuming. The commercially available defined substrate technologies Colilert and

Enterolert manufactured by IDEXX Laboratories, Inc. (IDEXX) are accepted by the U.S. Environmental Protection Agency as more convenient and less costly compared to traditional multiple-tube fermentation and membrane filtration methods for assessing fresh, marine, and estuarine surface waters (US EPA, 2003). As a result, IDEXX kits have become more popular in the past two decades around the world.

In 2000, the Clean Water Act was amended by the Beaches Environmental Assessment and Coastal Health (BEACH) Act. This law was designed to reduce the risk of disease to users of the U.S.'s coastal recreational waters, including the Great Lakes and waters adjacent to beaches (BEACH Act, 2000). The Act required the implementation and/or expansion of routine water quality monitoring in all U.S. specified waters by 2004 (BEACH Act, 2000). In preparation for this new standard, Wisconsin communities investigated the use of IDEXX Colilert-18 Quanti-Tray/2000 as a method to more efficiently and accurately test water quality (Kinzelman et al., 2005). Over a 2-year period, a study compared IDEXX to the traditional membrane filtration method of using mTEC agar to measure *E. coli* in 234 samples from 5 freshwater beaches. Using IDEXX decreased time from sample collection to public notification by at least 6 hours (18 hours vs. 24+ hours). Statistical analysis showed no significant difference between the data collected from both methodologies, with the 2 methodologies showing a strong positive correlation. Based on their results, the study concluded that IDEXX can be an acceptable alternative to the traditional membrane filtration technique for monitoring *E. coli* in recreational freshwater. A separate study compared IDEXX to two commonly used membrane filtration methods for samples from the Middle Rouge River, and found that *E. coli* counts were significantly correlated among the 3 methods (Vail et al., 2003).

While several other studies have also verified the use of IDEXX as an acceptable method for enumerating *E. coli* from drinking water, source water, and wastewater, few studies worldwide have compared IDEXX to traditional membrane filtration methods for recreational ocean waters to date (Edberg et al., 1990; Rice et al., 1990; Edberg et al., 1991; Fricker et al., 1995; Barrell et al., 1997; Eckner 1998; Graham 1999). Furthermore, despite IDEXX's relative ease of use and low cost, there are some notable drawbacks. The method can introduce user bias by relying on visual counts of positive wells, and it is known to have associated specificity issues (Ferguson et al., 2013). These tests are collectively called "defined substrate tests" since they measure the ability of organisms to metabolize a specific labeled substrate, releasing a

chromogen. For Colilert, total coliforms and *E. coli* are indicated by a yellow or a yellow and fluorescent metabolite, respectively. For Enterolert, enterococci are indicated by a fluorescent metabolite. The accuracy and dependability of IDEXX rely on the assumption that most non-target bacteria lack the required enzyme to metabolize the provided carbon source, making them unable to grow. A complete understanding of the assay microbiology, however, requires culture-independent analysis of the enrichments (Sercu et al., 2011).

In a study using samples from an urban creek in Santa Barbara, false-positive rates of FIB fell between 4-23% (Sercu et al., 2011). These results demonstrated how a variety of non-target bacteria taxa were detected in positive Colilert and Enterolert wells, which weren't detected in previous studies of the area using traditional culture-based techniques. These false positive Colilert or Enterolert readings can occur when there is an abundance of non-target bacteria that enzymatically cleave the chromogenic or fluorogenic substrates (Sercu et al., 2011). In 2018, a Netherlands ballast water test facility found that IDEXX Enterolert was grossly overestimating enterococci when *B. licheniformis* was present (Peperzak & van Bleijswijk, 2021). The researchers communicated the false-positive effect of *B. licheniformis* on Enterolert to IDEXX in hopes of the company improving the method's ability to enumerate enterococci in seawater. While monitoring the marine waters of Pinellas County in Florida, estimates of *E. coli* numbers using IDEXX Colilert frequently exceeded fecal coliform counts by membrane filtration by 1 to 3 orders of magnitude (Pisciotta et al., 2002). Overall, defined substrate technologies like IDEXX have been found to be more sensitive, with higher values obtained compared to membrane filtration, by multiple studies (Ramoutar, 2020). Based on these factors, it is important to consider the impact of possible false positives on the overestimation of FIB measurements in samples.

## **2.8 - IDEXX method and antibiotic-resistant bacteria**

Data on the significance of environmental contamination with antibiotic-resistant *E. coli* for human health are limited, reflecting the lack of a convenient detection method. While there is a body of literature validating IDEXX as a method for measuring FIB, its use in enumerating ARB has yet to be comprehensively explored. One study sampled 5 beaches in the Galapagos Islands to compare ocean water with and without discharge of human sewage (Overbey et al., 2015). IDEXX Enterolert was used to quantify enterococci, but antibiotic resistance testing was

performed on *E. coli* isolated by membrane filtration. Enterococci cultured by the Enterolert method were not used for antibiotic resistance testing because: (1) the test relies on growth of bacteria in a culture broth that likely selects certain bacteria while masking other strains that may have been present; (2) the method is capable of enriching a number of different *Enterococcus* species and sometimes non-Enterococcal bacteria (Ferguson et al., 2013), so that additional steps would have been necessary to isolate and speciate bacteria prior to antibiotic susceptibility testing; and (3) Enterococci are often intrinsically resistant to a number of antibiotics due to chromosomal resistance genes (Huycke et al., 1998; Jain & Marothi, 2014).

Another study explored antibiotic resistance of bacteria after WWTP effluent enters a stream, and chose to add antibiotics to Colilert as a rapid detection method for levels of antibiotic-resistant coliform bacteria and *E. coli* (Akiyama & Savin, 2010). Because the addition of antibiotics is a new use of Colilert, the researchers isolated the *E. coli* to confirm that bacteria identified as *E. coli* were in fact resistant to the selected antibiotics. Antibiotic-resistant *E. coli* were isolated from IDEXX Colilert tray wells positive for the growth of *E. coli* in the presence of a particular antibiotic. Samples were then streaked onto Mueller–Hinton agar plates containing the corresponding antibiotic and incubated at 37 °C for 16 to 18 hours. Putative antibiotic-resistant *E. coli* isolates were confirmed as *E. coli* using Gram staining and a commercially available Gram-negative bacteria identification kit. Another study similarly modified the IDEXX method to enumerate antibiotic-resistant *E. coli* in hospital effluent samples (Galvin et al., 2010). Antibiotics were added to Colilert Quanti-Trays and incubated. Samples of the fluid were then isolated and confirmed for *E. coli* presence. Lastly, antimicrobial susceptibility testing was performed using disc diffusion methods to confirm that positive IDEXX wells reflected growth of the target antibiotic-resistant *E. coli*.

## **2.9 - Remote sensing as a tool for digital water quality monitoring**

As mentioned, routine *in situ* water sampling can be costly and logistically challenging. Fueled by advancements in satellite imaging capabilities, the use of satellites in monitoring water quality is becoming a popular complementary tool to bolster sampling efforts. Monitoring water quality with remote sensing can provide real-time water quality reports that would otherwise be inaccessible. While traditional *in situ* monitoring will continue to be important, it is limited to point-based representations of highly complex and often spatially variable systems. Satellite

observations enable “supra-regional” monitoring, providing a time series of spatially comprehensive snapshots of a limited, but important set of water quality parameters. These parameters include turbidity, chlorophyll-a concentration, phycocyanin concentration, TSS, colored dissolved organic matter (CDOM), water surface temperature, and surface water roughness (Sent et al., 2021).

Landsat and Sentinel satellites are two popular families of satellites that currently carry out continuous remote sensing. Since the beginning of the program in the 1970s, a total of 9 Landsat satellites have been launched by NASA, with Landsat-9 being the newest member of the family as of 2021 (NASA, n.d.). The Sentinel satellites were designed and launched by the European Space Agency (ESA, n.d.b) to support the Copernicus Program- an Earth observation project developed by the European Union (ESA, n.d.a). Both families of satellites conduct remote sensing of Earth’s surface and gather geographical data to support global efforts in resource management, agriculture, and natural disaster response.

To conduct water quality assessments based on remote sensing data, the source of the satellite data must first be determined. While many data sources are available, Landsat-8 and Sentinel-2AB are two currently popular choices because of their global coverage (ESA, n.d.b; NASA, n.d.). Landsat-8 and Sentinel-2AB both have multispectral sensing capabilities, and the breadth of their spectral bands is very similar (USGS EROS Center, 2019). Multispectral sensing passively captures the electromagnetic waves reflected by the Earth’s surface, which can be inhibited during cloudy days and at night (Schulte to Bühne & Pettorelli, 2018).

Sentinel-2 is composed of two identical satellites: Sentinel-2A and Sentinel-2B that are arranged opposite each other on the orbital (ESA, n.d.b). Similar to the purpose of the Operational Land Imager (OLI) instrument in Landsat-8, the Multispectral Instrument (MSI) on Sentinel-2AB passively collects sunlight reflected from the Earth’s surface for different wavelength bands (ESA, n.d.b). Sentinel-2A and Sentinel-2B have trivial differences in the range of wavelengths detected by their respective bands. Both satellites have 13 different bands with a spatial resolution between 10 and 60 meters, with 20 meters being the most common resolution among all bands (ESA, n.d.b).

One difference between Landsat-8 and Sentinel-2AB is that Landsat-8 has additional capabilities with the installment of a Thermal Infrared Sensor instrument (TIRS). Sentinel-2AB can only measure short-wave infrared (SWIR) as its upper bound for detection ends at 2202.4 nm

(ESA, n.d.b). In comparison, the TIRS on Landsat-8 produces two bands spanning between 10.60-11.19  $\mu\text{m}$  and 11.50-12.51  $\mu\text{m}$  (NASA, n.d.). These two additional bands enhance wavelength atmospheric correction and the accuracy of surface temperature and emissivity (Roy et al., 2014). Additionally, Sentinel-2AB has a shorter revisit time compared to Landsat-8. Each Sentinel-2 satellite revisits every 10 days, and constellation with both Sentinel-2A and Sentinel-2B occurs every 5 days (USNA, 2021). In comparison, each Landsat satellite revisits every 16 days, and constellation with both Landsat-8 and Landsat-9 occurs every 8 days (USNA, 2021).

Due to the satellites' multispectral sensing being greatly compromised due to weather events, the raw band data has to be processed before use (Schulte to Bühne & Pettorelli, 2018). The raw Landsat-8 and Sentinel-2AB data usually go through radiometric and atmospheric correction before being used to calculate water quality metrics (Bonansea et al., 2019; Gonzales et al., 2018; Y. Wang et al., 2004). The radiometric correction transforms the numeric values of each pixel into absolute measurements of radiation per unit of light (Gonzales et al., 2018). Atmospheric correction refers to the process of eliminating atmospheric effects on the remote-sensing data (Gonzales et al., 2018). The data can also be preferentially selected or excluded depending on various conditions and criteria. For example, some studies only use days with little cloud coverage and no special weather events in their samples (Lim & Choi, 2015). Surrounding areas of artificial structures can also be excluded to ensure accurate analysis (Lim & Choi, 2015). After performing data transformation, different algorithms are used to compute numeric values of the desired water quality metrics. Once the calculated water quality metrics are obtained, appropriate regressions are usually run to examine correlations between the remote sensing data and *in situ* data (Toming et al., 2016).

In conclusion, multispectral satellites like Landsat-8 and Sentinel-2AB are popular choices for remotely sensing water quality because of their wide band range and easily accessible data. Today, it is widely recognized that satellite observations may be valuable for improving water quality monitoring and informing early warning systems. However, ground-truthing of water quality still presents methodological and modeling challenges since satellite data has relatively coarse resolution compared to water samples. Moving forward, a key challenge of remote sensing is translating satellite signals into meaningful ground-level contaminant detection that in turn, can inform water quality management decisions in real-time.

### 3. RESEARCH QUESTIONS

Satellite data are currently underutilized for water quality monitoring and public health protection. Even though remotely-sensed data are being collected around the globe every day, the potential uses for these data are just starting to be understood. A major obstacle is the paucity of data providing “ground-truthing” of satellite reflectance data. Our project aims to explore this research gap and combine microbial water quality analysis with space-based remote sensing. Our team collected *in situ* water samples from recreational coastal waters at times coincident with Sentinel-2AB and Landsat-8 satellite overpass times. We analyzed the water samples for standard water quality indicators including fecal bacteria and turbidity, as well as antibiotic-resistant pathogens, and examined relationships between different methodologies used. Our primary research questions included:

1. How well do *in situ* water samples correlate with satellite-derived turbidity data across Los Angeles coastal waters?
2. For *in situ* samples, how does the “gold standard” plate-based method for assessing *E. coli* and ARB compare to the more novel IDEXX method?

A strong correlation between satellite-derived turbidity values and other water quality metrics measured in lab would support the use of satellite data as a useful and efficient proxy for coastal water quality monitoring in real-time. Similarly, a strong correlation between the two methods for enumerating *E. coli* and ARB would validate IDEXX as an alternative to the plate-based method (hereafter referred to as “filter-plating” or “plate” method) for future microbiology research. Through these investigations, we ultimately hope to better understand how we can monitor water quality both accurately and efficiently with the physical and digital tools available.

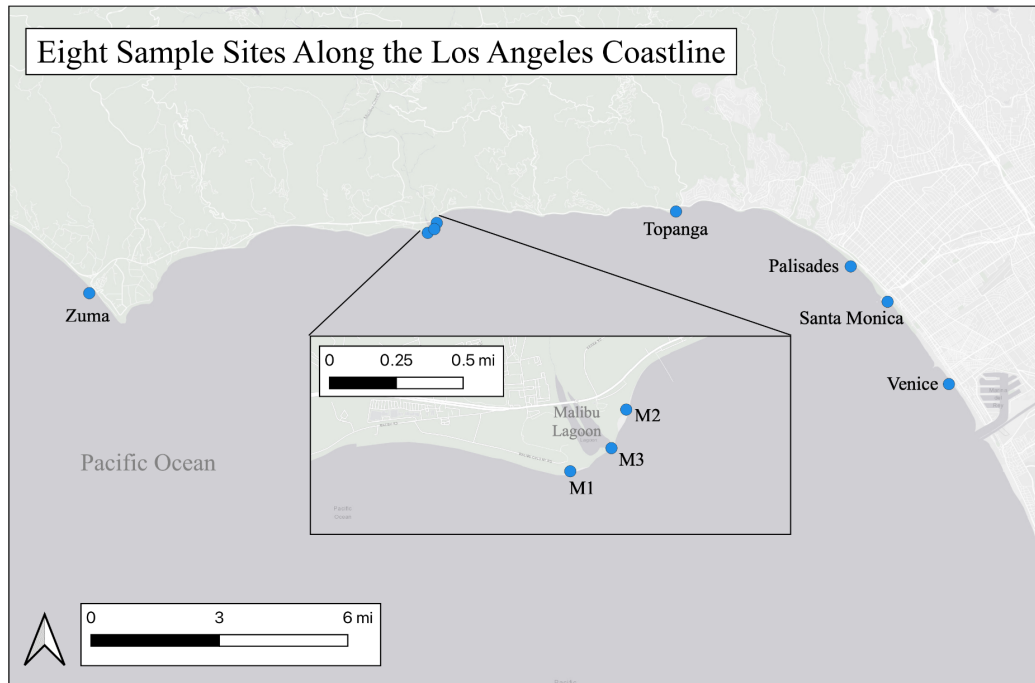
## 4. METHODS: WATER QUALITY

### 4.1 - On-site measurements

During satellite overpass days, water samples were collected between the time window of 10:15 AM - 1:15 PM. Six liters of water were collected in knee-deep water from each beach site at the coordinates listed below (Table 2). Sample bottles were labeled with the date and location, kept on ice, and transported back to the lab within three hours. Generic temperature and pH probes, as well as a turbidity meter, were used to record values on-site at the time of collection. Turbidity measurements taken on-site were assumed to be the “true” turbidity values and are hereafter referred to as “on-site probe turbidity”.

**Table 2.** Sample sites with coordinates of where water samples were collected.

Site	Latitude	Longitude
Venice Beach	33.98038383	-118.4705925
Santa Monica Beach	34.00718214	-118.4947045
Palisades Beach	34.01979456	-118.5097567
Topanga Beach	34.0382322	-118.5816725
Malibu Beach 1	34.03028693	-118.6818443
Malibu Beach 2	34.033797	-118.67951
Malibu Beach 3	34.031903	-118.6796
Zuma Beach	34.01101746	-118.819056

**Figure 1.** Map of 8 coastal sample sites.

### Turbidity meter (Appendix A)

A Thermo Scientific Orion AQUAfast AQ3010 Turbidity Meter was taken to each sampling site to obtain turbidity values in the field. Values were reported by the meter in Nephelometric Turbidity Units (NTU). A clean, dry sample vial was handled by the top cap and rinsed with 10 mL of sample water three times. On the fourth fill, the vial was capped with 10 mL of sample water and wiped dry with a soft, lint-free cloth. A thin film of silicone oil was then applied and wiped around the vial. The vial was then inserted into the sample well of the meter for measurement by aligning the arrow on the meter with the arrow on the outside of the vial. The meter was then turned on, the “Read/Enter” button was pushed, and the measured value was recorded.

## ***4.2 - In-lab measurements***

### Hydrolab readings

A Hydrolab HL4 Multiparameter Sonde was used to measure pH, turbidity, conductivity, and % dissolved oxygen for each sample. Turbidity and pH were measured using more than 1 device in our project to gather more comprehensive data.

### Total suspended solids (Appendix B)

Three 1.5  $\mu\text{m}$  filters were used to measure TSS for each site. Before use, filters were washed, baked for sterilization, and stored in a desiccator until needed. Initial weights of each filter were recorded immediately before running sample water through them. Then, a funnel manifold was set up with suction, and filters were sealed on with deionized water. Between 100 mL-600 mL of sample water was passed through each filter. Final calculations of weight accounted for the exact volume used. The filters were removed with tweezers, placed on individual aluminum pans, and dried for 24 hours in an oven. Lastly, filters were cooled in a desiccator and final weights were recorded.

### Light absorbance (Appendix C)

A spectrometer paired with the UV Express software were used to obtain light absorbance data. A baseline reading was established by adding 1 mL of MilliQ water to a glass cuvette in the spectrometer. After getting the baseline, a sampling cuvette was prepared and filled with 1 mL of sample water. Each sample was run from a frequency of 1100 nm-190 nm, and the sampling cuvette was rinsed 3 times with MilliQ water between each sample. After testing all of the samples, the data were exported from the software and saved.

### Nitrate (Appendix D)

All square sample cells were cleaned with detergent and rinsed with deionized water before use. The “351 N, Nitrate LR” test was selected on the LAMBDA 365 UV/Vis Spectrophotometer. A 25 mL graduated mixing cylinder was filled with 15 mL of sample water, and one NitraVer 6 Reagent Powder Pillow was added. The cylinder was closed, vigorously shaken for 3 minutes, and then left to rest for 2 minutes. After the 2 minutes, 10 mL of the solution was added to a clean square sample cell. One NitriVer 3 Reagent Powder Pillow was then added to this cell and gently shaken for 30 seconds. The sample cell was then left to rest for a reaction period of 15 minutes during which a pink color appeared if nitrate was present in the sample. While the 15-minute reaction period elapsed, a new square sample cell was filled with 10 mL of the sample water and ran to zero the spectrophotometer. After 15 minutes, the prepared

sample was run through the spectrophotometer. The detectable range for this test is from 0.01-0.50 mg/L.

### Ammonia (Appendix E)

All square sample cells were cleaned with detergent and rinsed with deionized water before use. The “385 N, Ammonia, Salic.” test was selected on the LAMBDA 365 UV/Vis Spectrophotometer. One square sample cell was filled with 10 mL of the sample while another was filled with 10 mL of deionized water. One Ammonia Salicylate powder pillow was added to each square sample cell. The square sample cells were then shaken enough to dissolve the reagent and left to rest for 3 minutes. After the 3 minutes, one Ammonia Cyanurate powder pillow was added to each sample cell, shaken until the reagent was dissolved, and then left to rest for 15 minutes. If ammonia was present, a green color would develop as the reaction occurred. Once 15 minutes had elapsed, the blank sample cell with the deionized water was wiped clean and ran to zero the spectrophotometer. The square sample cell was then wiped, inserted, and read to show results in mg/L of  $\text{NH}_3\text{-N}$ . The detectable range for this test was from 0.01-0.50 mg/L.

### Phosphorus (Appendix F)

Prepared sample tubes with the PhosVer 3 Phosphate reagent were labeled for each sample site. The “Phosphorus, Reactive (Orthophosphate)” test was used on the LAMBDA 365 UV/Vis Spectrophotometer with a light shield in cell compartment 2. 5.0 mL of sample water was added to the appropriate Test ‘N Tube Vial, capped, and mixed. The vial was wiped clean and inserted into the 16 mm round cell holder to zero the spectrophotometer. One PhosVer 3 Phosphate Powder Pillow was added to the sample, capped, and shaken for 20 seconds. After two minutes, the tube was placed inside the spectrophotometer. The detectable range for this test is from 0.06-5.00 mg/L.

## **5. METHODS: FECAL INDICATOR BACTERIA**

### ***5.1 - IDEXX method***

The IDEXX method for enumerating FIB was performed according to the manufacturer’s instructions (Appendix G). Total coliforms (TC) and *E. coli*, antibiotic-resistant coliforms and

ESBL-*E. coli*, and enterococci were measured for each sample site, equating to 3 solutions prepared for analysis per site. Solutions were prepared by adding chemical substrates (Colilert-18 and Enterolert reagent packets) to a 1:10 dilution ratio of sample water to MilliQ water. This dilution ratio was based on historical ocean water quality data and allowed for countable results. To measure antibiotic-resistant coliforms and ESBL-*E. coli*, 100  $\mu$ L of cefotaxime antibiotic syrup was added to one of the solutions. The final solutions were then poured into Quanti-Trays and sealed for incubation. After incubating the Colilert trays for 18-22 hours at 35°C and the Enterolert trays for 24 hours at 41°C, the samples were examined for the presence of yellow color or fluorescence. Coliforms were indicated by yellow wells, while *E. coli* and enterococci were indicated by fluorescence under UV light. A most probable number (MPN) table provided by IDEXX was used to convert the number of wells positive for fluorescence or yellow color to the MPN of bacteria (CFU/100 mL). This value was then compared to manual colony forming unit (CFU) counts from the filter-plating method.

## **5.2 - Filter-plating method** (Appendix H)

### Media preparation

Phosphate Buffered Saline (PBS) Preparation: 2.5 g disodium hydrogen phosphate, 0.58 g sodium dihydrogen phosphate, and 8.5 g sodium chloride were mixed into 1 L of reagent grade water and autoclaved at 121°C for 15 minutes.

Cefotaxime Antibiotic Preparation (50 mg/mL): 250 mg of cefotaxime sodium salt was and 250 mg antibiotic solution were added to 5 mL of reagent grade water. The cefotaxime antibiotic solution was divided into 50  $\mu$ L aliquots and stored in PCR tubes at -20 °C.

mTEC Agar Plate Preparation (for 40 to 50 plates): A solution of 9.12 g modified mTEC agar powder and 200 mL reagent grade water was autoclaved at 121 °C for 15 minutes and then cooled to 40-50 °C using a temperature bath. Once cooled, half of the agar media (100 mL) was transferred to an Erlenmeyer flask and spiked with 8  $\mu$ L of cefotaxime antibiotic stock solution. The antibiotic spiked media was poured into 50 mm plates (4 mL per plate) and labeled with “(+)” For the control plates without antibiotic, the remaining 100 mL of mTEC agar media was poured into 50 mm plates (4 mL per plate) and labeled “(-).”

### Testing media with positive and negative controls

First, the Positive antibiotic-resistant control (*E. coli* BAA-2326 (ESBL-producing)) was streaked on mTEC agar with cefotaxime, and colony growth and morphology were observed. Next, we streaked Positive antibiotic-resistant control (*E. coli* BAA-2326 (ESBL-producing)) on mTEC agar and observed morphology and colony growth while comparing it to no growth after streaking on mTEC agar with cefotaxime. Lastly, the negative control (*Enterococcus faecalis* ATCC 19433) was streaked on the mTEC agar plate where no growth should be seen.

### Membrane filtration

A 0.45 µm membrane filter was placed in a filter cup, followed by a 0.20 µm membrane filter. Then, 30 mL of PBS followed by 3 sequential dilutions of sample water were added and vacuumed through the filter cup. The sides of the filter cup were rinsed with 5-10ml of PBS, and the 0.20 µm membrane was discarded. Finally, the 0.45 µm filter was transferred onto an mTEC agar plate. This process was completed 4 times for each sample site, producing two antibiotic spiked (+) plates and two control (-) plates.

Two method blanks were created similarly. For the blanks, 100 mL of PBS was filtered through the membranes before the transfer of the 0.45 µm filter onto an mTEC agar plate. Finally, the Petri dishes were closed, inverted, and incubated in a sealed ziplock bag at 44.5°C ± 0.2°C for 22 ± 2 hours.

### Plate counting and analysis

After incubation, a countable dilution was used and compared with the number of purple colonies (bacteria CFU) on each plate to obtain a value for the average *E. coli* CFUs/100mL of sample water.

$$\frac{E. coli}{100 mL} = \frac{\text{Average } E. coli \text{ colonies at countable dilution}}{\text{Volume of sample filtered (mL)}} \times 100$$

By dividing the total number of cefotaxime-resistant *E. coli* by the total of *E. coli* for each sample, we obtained the proportion of *E. coli* that is resistant to cefotaxime.

$$\% \text{ Cefotaxime - resistant } E. coli = \frac{\text{CFU of Cefotaxime - resistant } E. coli / 100 mL}{\text{CFU of total } E. coli / 100 mL} \times 100$$

## 6. METHODS: REMOTE SENSING AND DATA ANALYSIS

### *6.1 - Remote sensing data acquisition*

#### ACOLITE (Appendix I)

Python 3.10.2, Anaconda Navigator, and ACOLITE (a generic atmospheric correction module) were used to analyze satellite images over our sample sites. First, remote sensing images were downloaded from USGS Earth Explorer from the Sentinel-2AB or Landsat-8 satellites for the date of interest. Cloud cover was restricted to 60%. The image was downloaded as a Level-1C Tile in JPEG2000 format. These images were then run through the ACOLITE interface to extract a .tif file. To obtain turbidity data, this file was run through a Python script to extract mean turbidity (in FNU) and standard deviation for each sample site.

#### Google Earth Engine (Appendix J)

Similar to the ACOLITE workflow, remotely-sensed images were imported into Google Earth Engine (GEE). On this interface, a Python script returns turbidity data (in NTU) for the sample area. Using the coordinates of each sample site, turbidity values were recorded and compared to ACOLITE results to investigate potential correlation.

#### Bakun Upwelling Index

Due to the impact seasonal weather could have on measured values, the relationship between the measured parameters and upwelling indices was also explored in our models. Data was obtained from NOAA's SWFSC Environmental Research Division using their "Upwelling Index, 33N 199W 6-hourly" database.

### *6.2 - Regression models for turbidity*

To analyze the satellite-derived turbidity values, simple linear regression (SLR), multiple linear regression (MLR), ridge regression, and random forest models were built. In the SLR model, Sentinel-2AB ACOLITE turbidity was chosen as the predictor variable and on-site probe turbidity was chosen as the dependent variable. The ACOLITE-derived turbidity data had a higher correlation with the turbidity data measured on-site after removing outliers, so it was used instead of the GEE-derived turbidity data in the SLR model. The initial SLR model was

constructed on all available data points, totaling 33 observations. Additionally, two methods were adopted to further reduce error in the model. The outliers, which are defined as observations that have a Cook's Distance greater than  $4/n$  and whose residuals are more than 3 standard deviations away from the mean, were removed. A K-means clustering analysis was also used to identify subsets of observations that could generate a stronger linear regression output. Both Sentinel-2AB ACOLITE turbidity and on-site probe turbidity were scaled prior to running the clustering algorithm.

For the MLR model, ridge regression model, and random forest model, a subset of 20 observations were used due to various missing values in our data. No imputation was conducted due to the small sample size. To select features for constructing the models, the availability of the data was first considered, and then features with relatively strong correlations were selected.

Due to the small sample size ( $n = 20$ ), the models were likely to exhibit overfitting. Hence, in all three multivariable models, a 4-fold cross-validation with 10 repeats was performed. The 4-fold cross-validation split the data into 75% training and 25% testing. Three metrics were selected to evaluate the performance of the multivariable models: Mean Absolute Error (MAE), Root Mean Square Error (RMSE), and the  $R^2$  value for the regression between the predicted and actual values.

Mean Absolute Error (MAE) is defined as: 
$$\sum_{i=1}^n |\text{predicted} - \text{actual}| * \frac{1}{n}$$

Root Mean Square Error (RMSE) is defined as: 
$$\sqrt{\sum_{i=1}^n (\text{Predicted} - \text{Actual})^2 * \frac{1}{n}}$$

### **6.3 - Comparison between IDEXX and filter-plating method**

To validate the accuracy of the IDEXX method against the filter-plating method, Simple Linear Regression (SLR) models were constructed to examine the relationship between the data gathered from both methods. Additionally, due to limited data on antibiotic-resistant *E. coli*, a chi-square test was used to examine the difference between the two methods in measuring percent antibiotic-resistant *E. coli*.

## 7. RESULTS

### 7.1 - Data collection and testing for correlations

We completed a total of twelve sampling days between January 28th, 2022, and May 23rd, 2022 on satellite overpass days. On each sampling day, we aimed to collect samples from all eight beaches. However, due to time and transport limitations, there were days we could only go to some of the beaches. Cloud cover was also a limitation. Nineteen water samples could not be compared to satellite data due to high cloud coverage during the satellite overpass time. Table 3 details each *in situ* sampling-satellite data match-up. Gray indicates no satellite data were obtained due to cloud cover. Purple indicates that both ACOLITE and GEE data were obtained from Sentinel-2AB, while blue indicates that only GEE values were obtained. Green indicates that ACOLITE data were obtained from Landsat-8. Due to Landsat-8's longer revisit time, we were only able to collect samples on two Landsat-8 overpass days. Since we ended up with such limited Landsat-8 data, we focused on Sentinel-2AB data in our final analyses.

**Table 3.** Satellite overpass day match-ups.

Too cloudy for satellites
  Landsat ACOLITE
  Sentinel GEE
  Sentinel ACOLITE/GEE

Date	Beaches Sampled							
01/28/2022	Venice	Santa Monica	--	--	--	--	--	--
01/30/2022	Venice	Santa Monica	Palisades	Topanga	Malibu 1	Malibu 2	Malibu 3	Zuma
02/07/2022	--	--	--	--	Malibu 1	Malibu 2	Malibu 3	Zuma
02/17/2022	Venice	Santa Monica	Palisades	--	Malibu 1	Malibu 2	Malibu 3	--
03/14/2022	Venice	Santa Monica	Palisades	Topanga	Malibu 1	Malibu 2	Malibu 3	Zuma
04/04/2022	Venice	Santa Monica	Palisades	Topanga	Malibu 1	Malibu 2	Malibu 3	Zuma
04/08/2022	Venice	Santa Monica	Palisades	Topanga	Malibu 1	Malibu 2	Malibu 3	Zuma
04/18/2022	Venice	Santa Monica	Palisades	Topanga	Malibu 1	Malibu 2	Malibu 3	Zuma
04/23/2022	Venice	Santa Monica	Palisades	Topanga	Malibu 1	Malibu 2	Malibu 3	Zuma
05/13/2022	Venice	Santa Monica	Palisades	Topanga	Malibu 1	Malibu 2	Malibu 3	Zuma
05/18/2022	Venice	Santa Monica	Palisades	Topanga	Malibu 1	Malibu 2	Malibu 3	Zuma
05/23/2022	Venice	Santa Monica	Palisades	Topanga	Malibu 1	Malibu 2	Malibu 3	Zuma

From sampling, we obtained a total of 65 satellite overpass match-up values. Figure 2 displays the correlation coefficients between all of the water quality metrics and methods we measured. Correlation coefficients were calculated based on the highest available number of observations for each pair of variables.

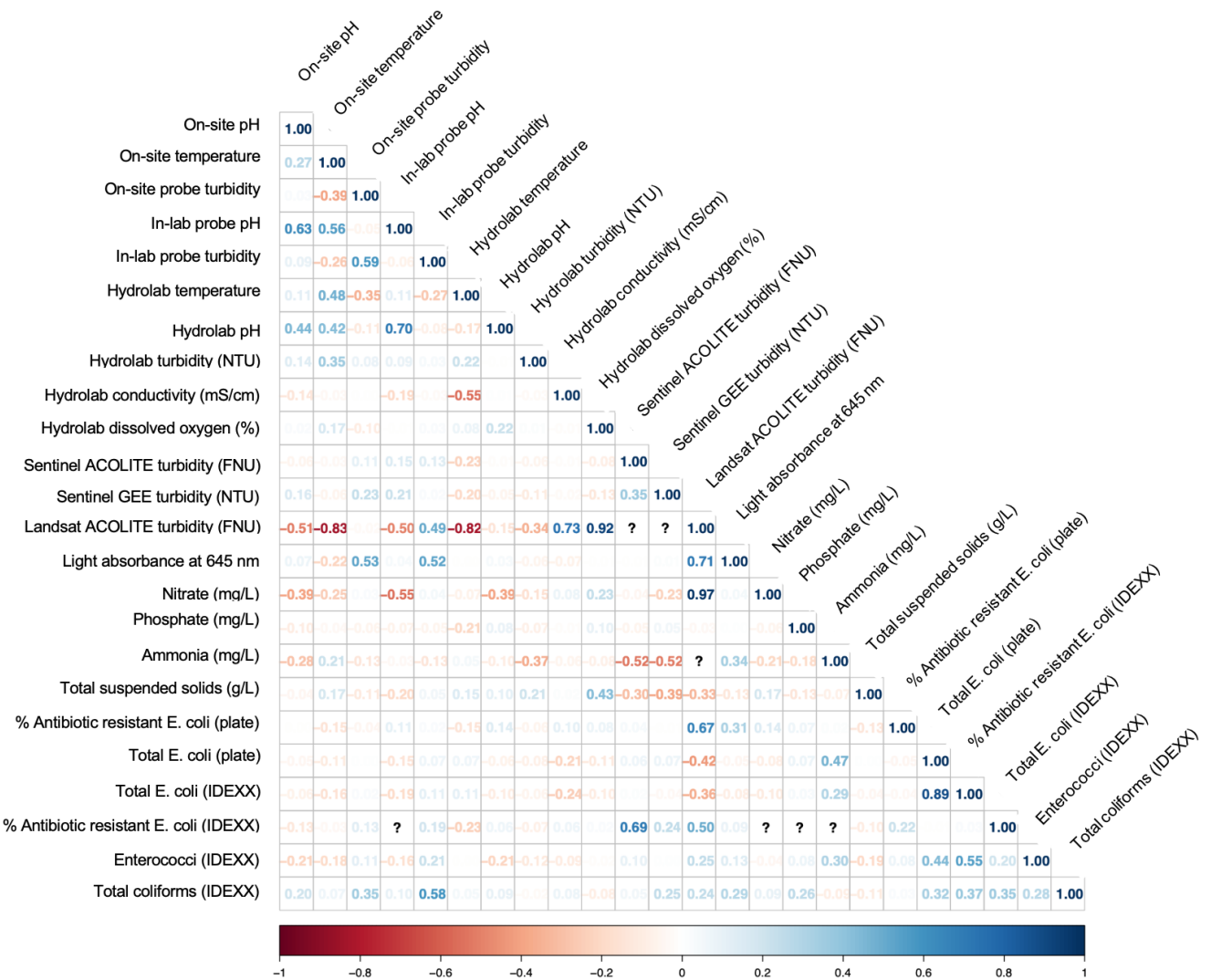


**Figure 2.** Correlation coefficient plot of all variables measured for water quality. All outliers included.

After removing outliers, the correlation coefficient between on-site probe turbidity and Sentinel-2AB ACOLITE turbidity was 0.624. Hydrolab measurements, pH, and light absorbance showed strong correlations with on-site probe turbidity. TSS and light absorbance are also included as features in the final model. Table 4 shows an overview of the complete model.

**Table 4.** Feature selection table of completed models.

Feature Category	Features	Target Variable
Remote Sensing Data	Sentinel-2AB GEE Turbidity	On-Site Probe Turbidity
	Sentinel-2AB ACOLITE Turbidity	
In-Lab Measurement	Hydrolab pH	
	Hydrolab % Dissolved Oxygen	
	TSS	
	Light Absorbance	
External	Upwelling	

### 7.2 - *Satellite-derived turbidity*

Sentinel-2AB turbidity values derived from ACOLITE and GEE were significantly correlated ( $n = 58, p = 0.005994$ ). With the removal of outliers, Sentinel-2AB ACOLITE turbidity was correlated with on-site probe turbidity ( $n = 38, p = 0.0203$ ) and in-lab probe turbidity ( $n = 42, p = 0.006299$ ). With the removal of outliers, Sentinel-2AB GEE turbidity was also correlated with on-site probe turbidity ( $n = 40, p = 0.003895$ ) and in-lab probe turbidity ( $n = 45, p = 0.03297$ ).

### 7.3 - *Simple linear regression for turbidity*

The initial SLR model does not show a statistically significant  $R^2$  value between Sentinel-2AB-derived turbidity and on-site probe turbidity, as the  $p$ -value of the F-test was 0.579 (Fig. 3a). After removing outliers, the  $R^2$  value increased to 0.39 with a  $p$ -value of 0.0001289 (Fig. 3b). Additionally, in the model without outliers, Sentinel-2AB ACOLITE turbidity was a statistically significant predictor of on-site turbidity values, as the estimated slope of the regression line was 0.7752 with a  $p$ -value of 0.00129. Table 5 summarizes the comparison between the two regression models.

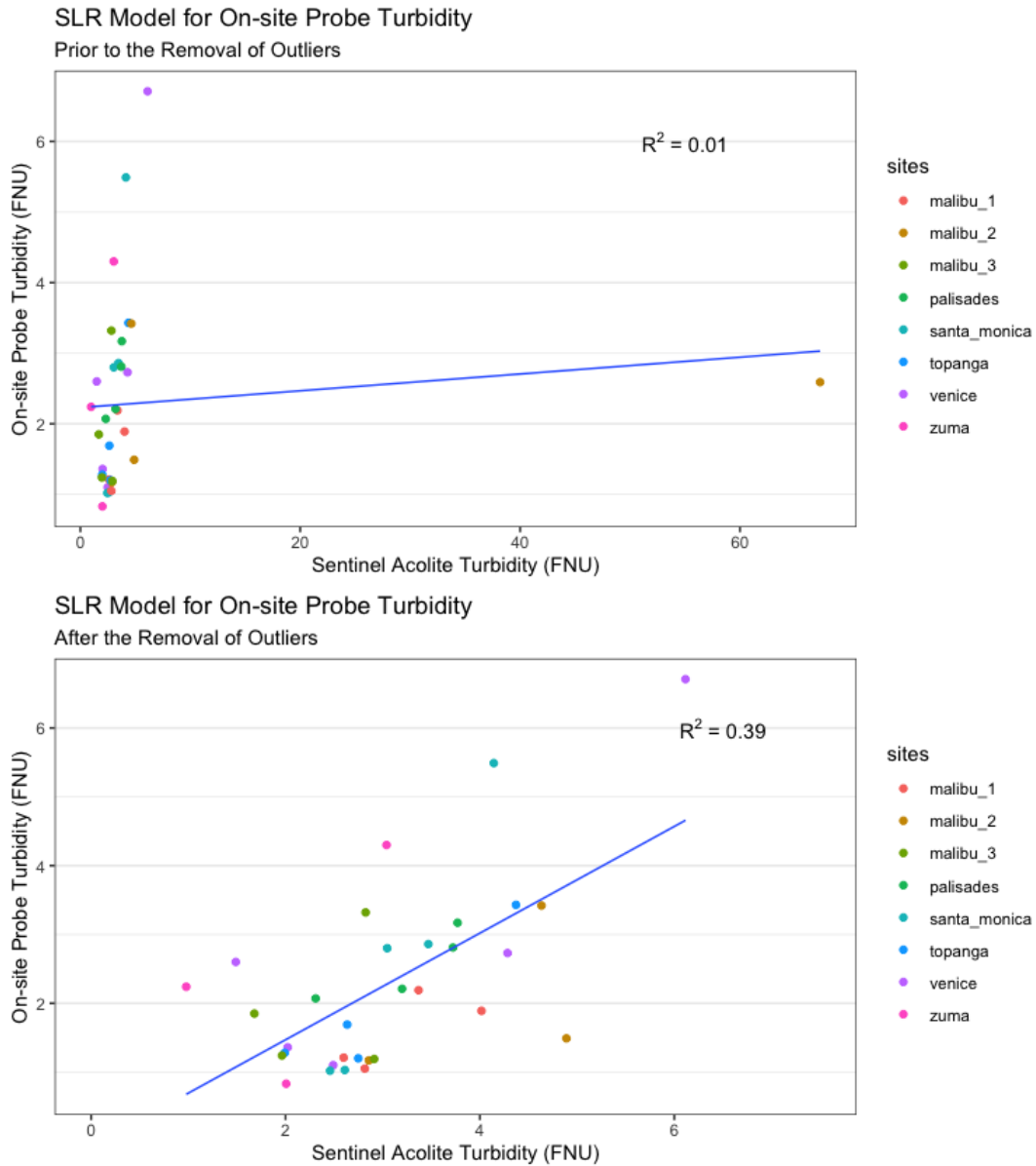


**Figure 3a/b.** Simple linear regression graphs before (a) and after (b) removal of outliers.

**Table 5.** Simple linear regression outputs before and after removal of outliers.

	SLR (M0)	SLR (outliers removed) (M1)
$\beta_0$ Intercept	2.230	-0.081
$\beta_1$ Slope ( $p$ -val)	0.012 (0.579)	0.775 (0.001) ***
$R^2$	0.010	0.391

A clustering analysis was also applied to the raw dataset to select for subsets of data where a more robust SLR model can be obtained. 4 clusters were determined to be optimal for minimizing the sum of squares in between clusters (Fig. 4a/b). After assigning each observation to one of the four clusters, an SLR model was built within the 2nd, 3rd, and 4th clusters as well as for the 2nd and 4th cluster combined data (Fig. 5a/b/c/d). Although the 3rd cluster produces the largest  $R^2$  value, the  $p$ -value of the slope indicated no statistically significant results as there was a relatively small degree of freedom (Table 6). The 2nd cluster produced the largest  $R^2$  value that was statistically significant among all of the subsets. The 4th cluster showed poor results with an  $R^2$  value of 0.01.

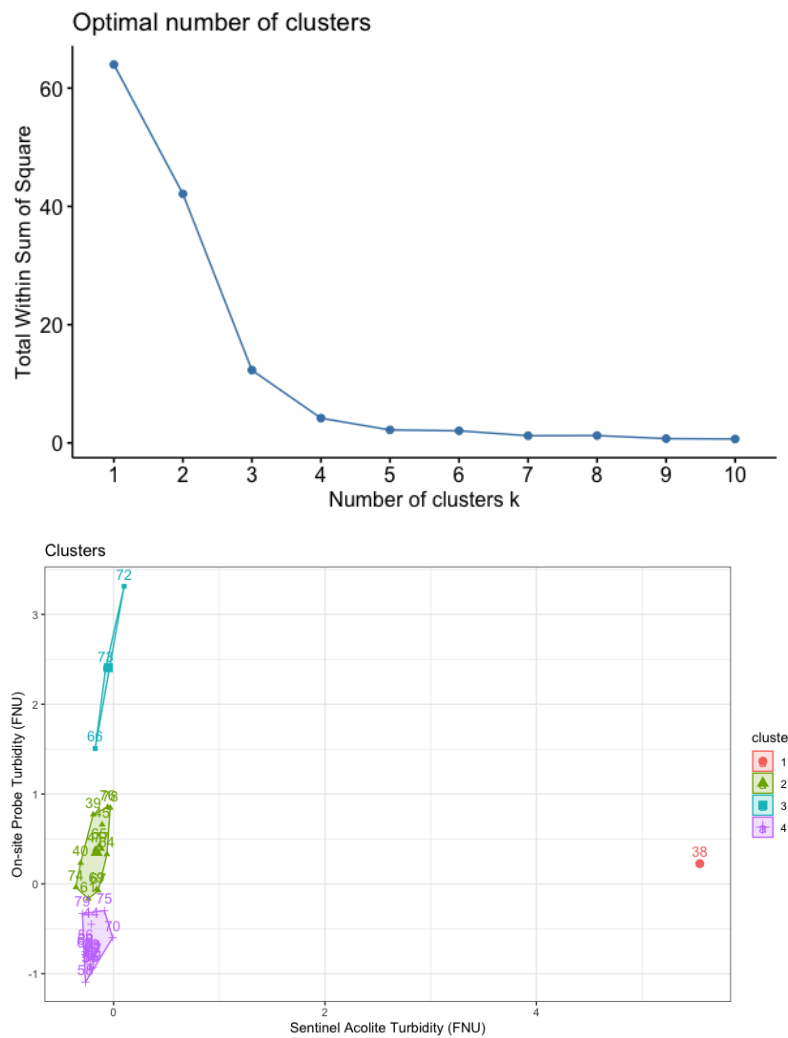


**Figure 4a/b.** Selecting the number of optimal clusters (a) & results of applying clustering analysis (b).

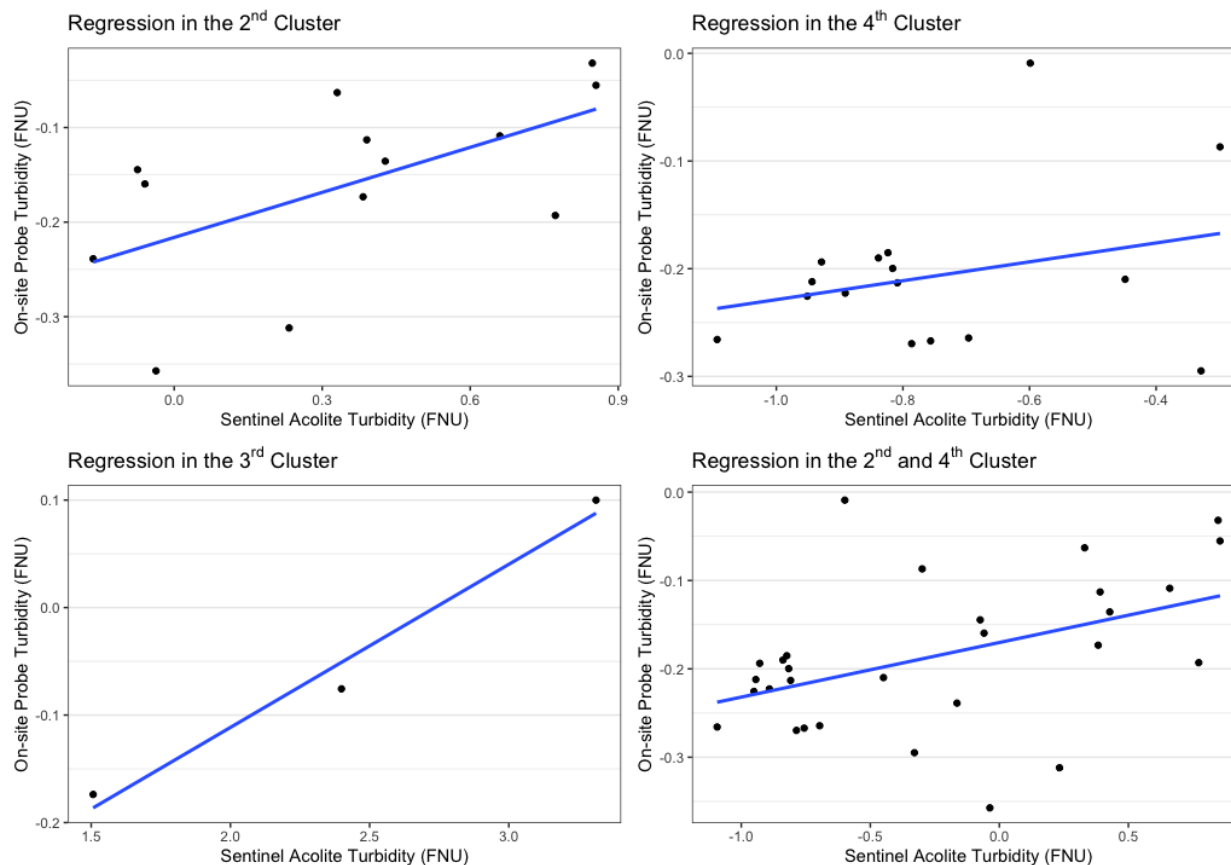


**Figure 5a/b/c/d.** Regression output in the 2nd (a), 3rd (b), 4th (c), and 2nd and 4th (d) combined cluster.

**Table 6.** Regression outputs of simple linear regression models in clusters.

SLR Models	2nd Cluster (M2)	3rd Cluster (M3)	4th Cluster (M4)	2nd & 4th Cluster (M5)
$\beta_0$ Intercept	-0.216	-0.415	-0.141	-0.170
$\beta_1$ Slope ( $p$ -val)	0.159 (0.033) ***	0.152 (0.098)	0.088 (0.300)	0.062 (0.013)*
R <sup>2</sup>	0.293	0.953	0.01	0.177

**7.4 - Multiple linear regression and ridge regression for turbidity**

Both the MLR model and the ridge regression model were cross-validated using a 4-fold method with 10 repeats. Table 7 reports the root mean square error (RMSE), the R<sup>2</sup> value from regressing the predicted values against the actual values, and the mean absolute error (MAE) averaged over the 10 repeats. For the ridge regression model, 1.6 was selected as the penalty term lambda because it yielded the R<sup>2</sup> largest value (Fig. 6).

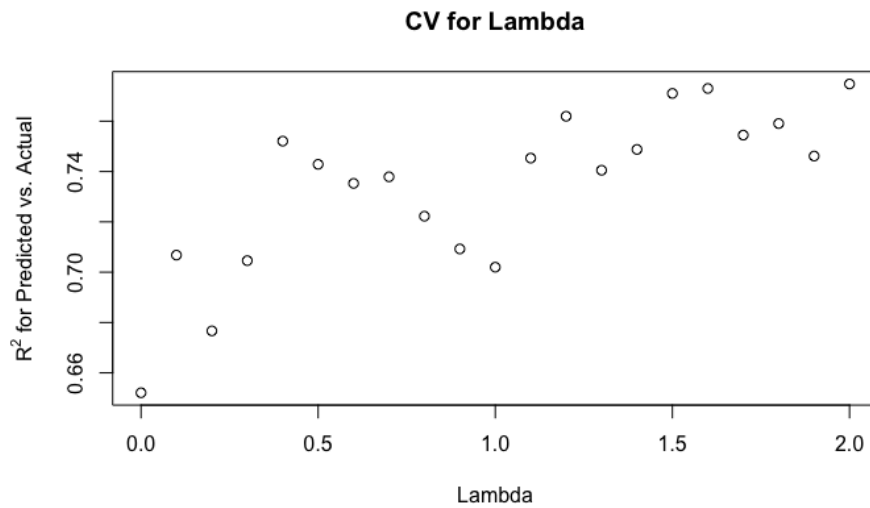


**Figure 6.** Selecting the optimal penalty term  $\lambda$  for ridge regression model.

**Table 7.** Comparing the regression outputs between multiple linear regression and ridge regression models.

	MLR Model	Ridge Regression Model ( $\lambda=1.6$ )
RMSE	1.189	0.916
R <sup>2</sup>	0.618	0.766
MAE	0.995	0.698

**7.5 - Random forest regression for turbidity**

The number of trees was cross-validated manually. 17 trees yielded the highest R<sup>2</sup> value (Fig. 7). After tuning the number of trees, the number of sample variables was tuned by the 4-fold validation with 10 repeats. The results are summarized in Table 8. The final Random Forest Regression was constructed with 17 trees and 2 variables were sampled as candidates at each split.

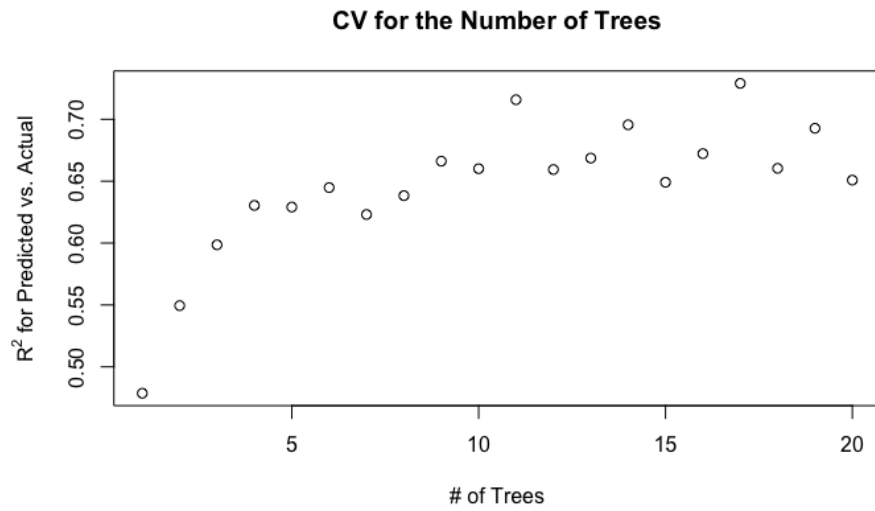


**Figure 7.** Selecting the optimal number of trees for random forest regression model.

**Table 8.** Selecting the optimal number of resample variables for random forest regression model.

# of Resampled Variables	RMSE	R <sup>2</sup>	MAE
2	1.077	0.653	0.797
4	1.103	0.631	0.805
7	1.122	0.640	0.840

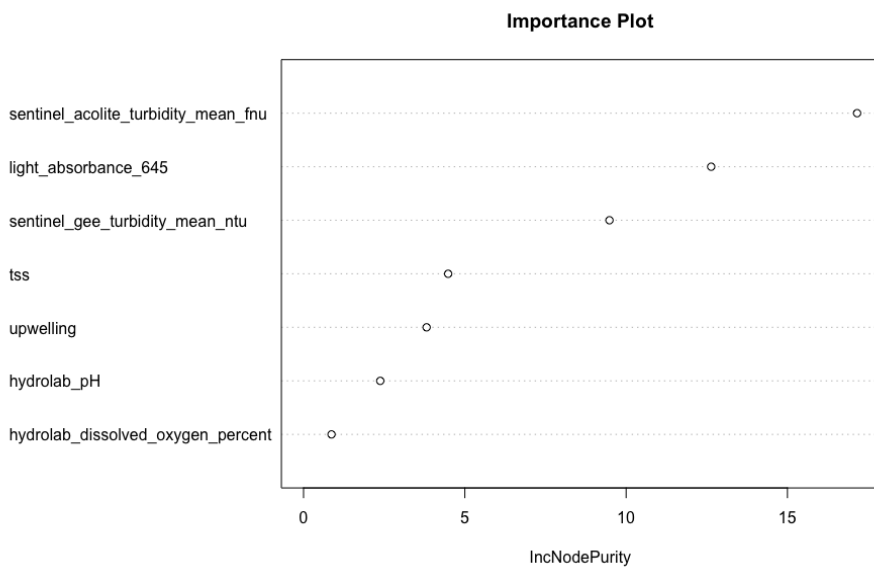


**Figure 8.** Importance plot of the random forest regression model.

### 7.6 - Additional water quality metrics

No statistically significant relationships were found between satellite-derived turbidity and the other water quality metrics measured, except for phosphorus levels. With the removal of outliers, Sentinel-2AB GEE turbidity was correlated with phosphorus ( $n = 32$ ,  $p = 0.01657$ ).

### 7.7 - IDEXX vs. filter-plating method

The two figures below display the relationship between the filter-plating and IDEXX methods for enumerating the percentage of antibiotic-resistant *E. coli* and total *E. coli* concentration in the samples. The  $R^2$  value for the regression in the percentage of antibiotic-resistant *E. coli* between the methods was 0.0466 ( $n = 43$ ,  $p = 0.1557$ ), while the  $R^2$  value for comparing *E. coli* concentration was 0.7825 ( $n = 69$ ,  $p < 0.0001$ ).

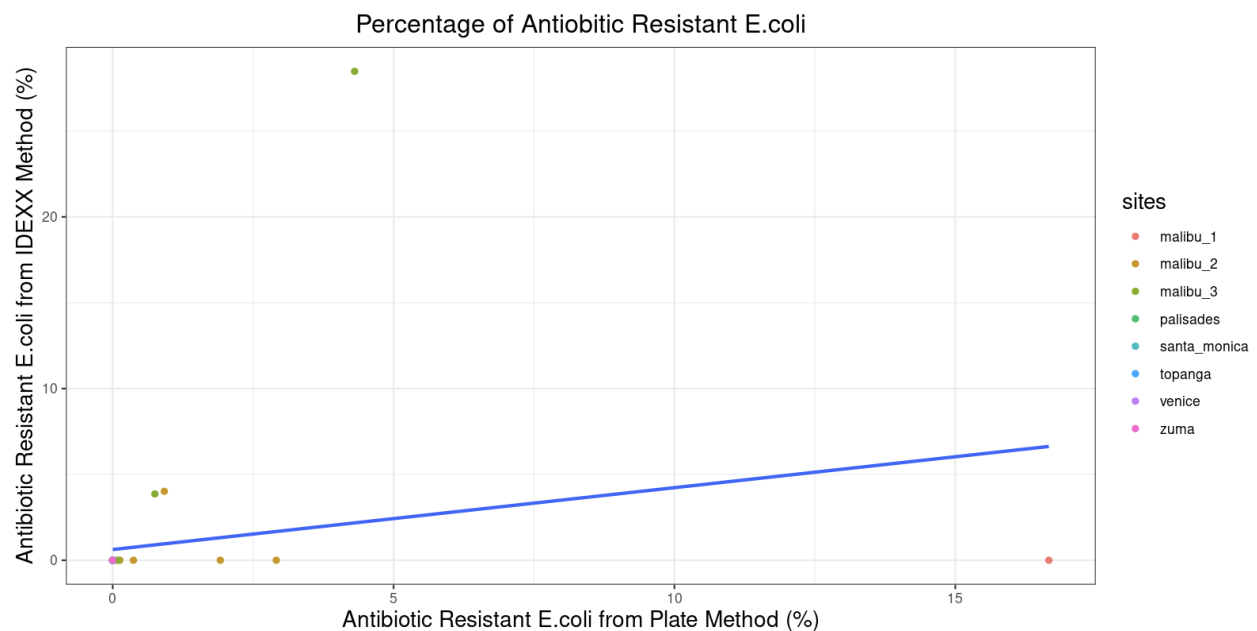


**Figure 9.** Simple linear regression model for comparing the IDEXX method and the filter-plating method in measuring the percentage of antibiotic-resistant *E. coli* in samples.

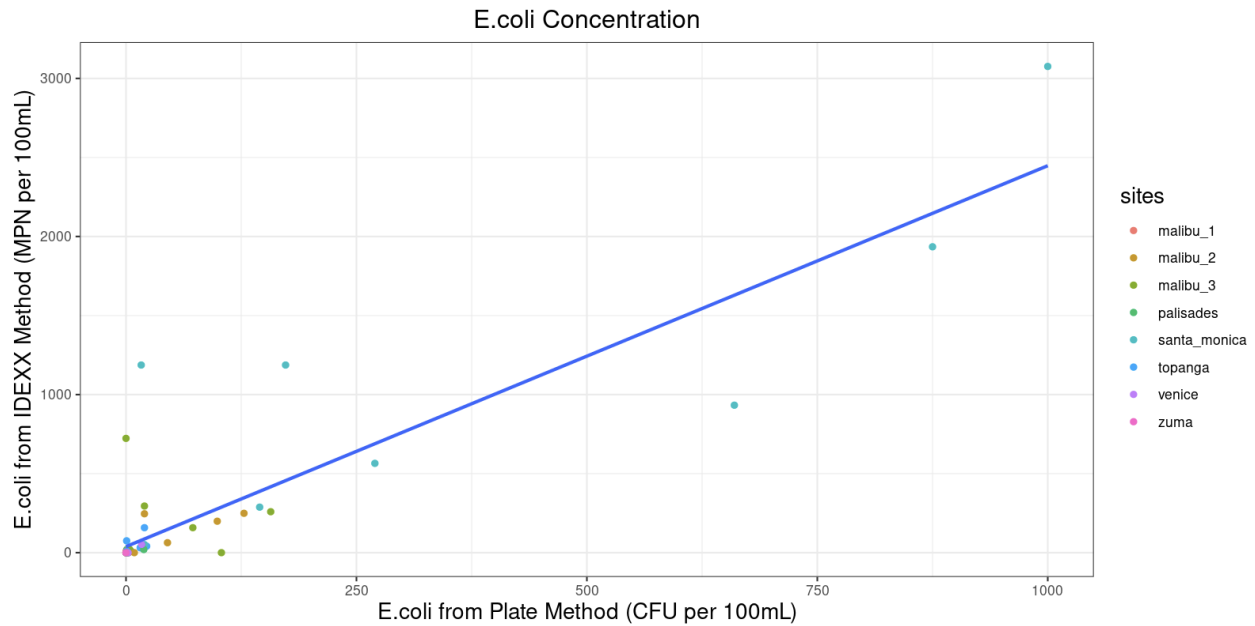


**Figure 10.** Simple linear regression model for comparing the IDEXX method and the filter-plating method in measuring the total concentration of *E. coli* in samples.

Table 9 displays the percentage of antibiotic-resistant *E. coli* in samples collected when analyzed categorically for both the filter-plating and IDEXX methods. Sample results were grouped into 3 categories: no antibiotic-resistant *E. coli* found, 0-20% of total *E. coli* are antibiotic-resistant, and more than 20% of total *E. coli* are antibiotic-resistant. The chi-square test yielded a significant *p*-value of 0.001911.

**Table 9.** Summary table of the number of samples with 0%, between 0% and 20%, and more than 20% antibiotic-resistant *E. coli*.

		IDEXX Method		
		0%	>0% & <20%	>20%
Plate Method	0%	35	0	0
	>0% & <20%	6	2	1
	>20%	0	0	0

### 7.8 - Fecal indicator bacteria vs. turbidity

With the filter-plating method, no statistically significant correlations were found between total *E. coli* or antibiotic-resistant *E. coli* and Sentinel-2AB ACOLITE/GEE turbidity. However, a correlation was found between in-lab probe turbidity and total *E. coli* after the removal of outliers ( $n = 54, p = 0.02845$ ).

With the IDEXX method, no statistically significant correlations were found between total *E. coli* or total coliforms and Sentinel-2AB ACOLITE/GEE turbidity. However, a correlation was found between antibiotic-resistant *E. coli* and Sentinel-2AB ACOLITE turbidity ( $n = 26, p < 0.0001$ ). Total coliforms were correlated with on-site probe turbidity ( $n = 51, p = 0.01217$ ). After the removal of outliers, enterococci had a weak relationship with Sentinel-2AB ACOLITE turbidity ( $n = 28, p = 0.05364$ ). Among all 3 of the tested FIB, *E. coli* and enterococci had the strongest correlation ( $n = 54, p < 0.0001$ ). Also, total coliforms were strongly correlated with *E. coli* ( $n = 62, p = 0.003054$ ) and enterococci ( $n = 50, p = 0.04858$ ).

### 7.9 - Spatial distribution of *E. coli*

The following boxplots show the spatial distribution of both total *E. coli* concentration and antibiotic-resistant *E. coli* across the 8 sample sites obtained from the filter-plating method. As shown in Figure 11, Santa Monica consistently had the highest levels of total *E. coli* ( $n = 9$ ). As shown in Figure 12, with the removal of one outlier from Malibu 1, Malibu 2 and 3 had the highest levels of antibiotic-resistant *E. coli* ( $n = 10$ ).

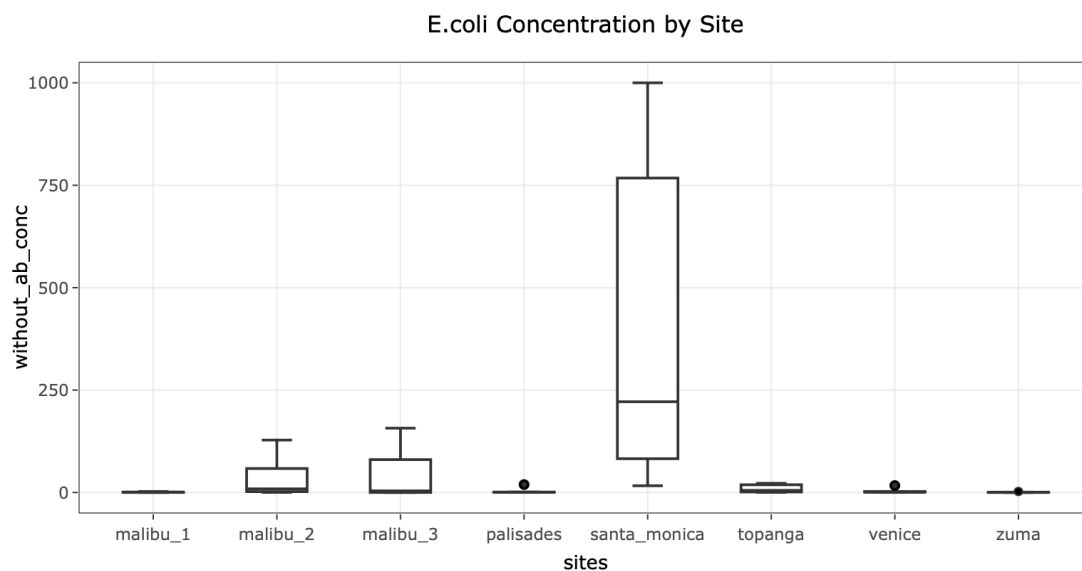


**Figure 11.** Distribution of *E. coli* concentration across all 8 sites.

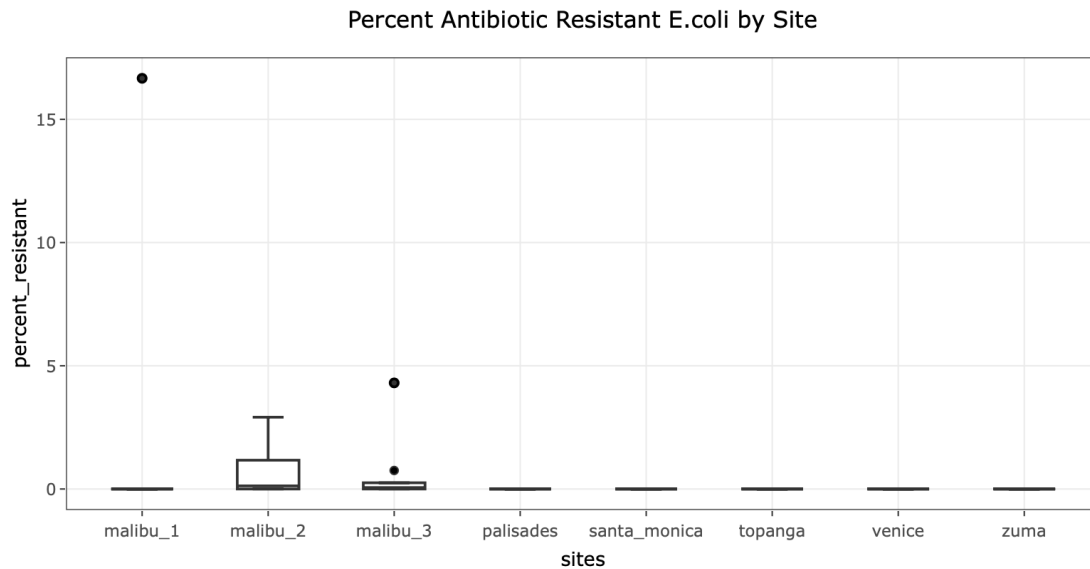


**Figure 12.** Distribution of antibiotic-resistant *E. coli* across all 8 sites.

## 8. DISCUSSION

### 8.1 - Simple linear regression for turbidity

Overall, both the removal of outliers and the clustering analysis improved the robustness of our model. The clustering analysis further indicates that the single linear regression model is strongest when the water is less turbid. The fact that most of the observations in M2 have negative values shows that the turbidity measured on-site is smaller than the mean turbidity across all observations. However, it is important to note that M4, which is also composed of on-site readings less than the mean, demonstrated a contrasting result where smaller than usual on-site turbidity is more difficult to predict with the remote sensing data. This can be attributed to the fact that in the 4th cluster, Sentinel-2AB ACOLITE turbidity values are all smaller than the mean. Thus suggests that if the Sentinel-2AB-derived reading is small, it is more difficult to predict the on-site reading. Overall, M1 and M2 are both more robust compared to the initial model M0. One slight advantage of M2 is that its average residuals are smaller. The residual vs. fitted plots reveal that M2 demonstrates better homoscedasticity compared to M1 as the residuals are more evenly distributed in the second residual vs. fitted plot compared to the first one. Still, M1 provides the largest  $R^2$  of 0.39.

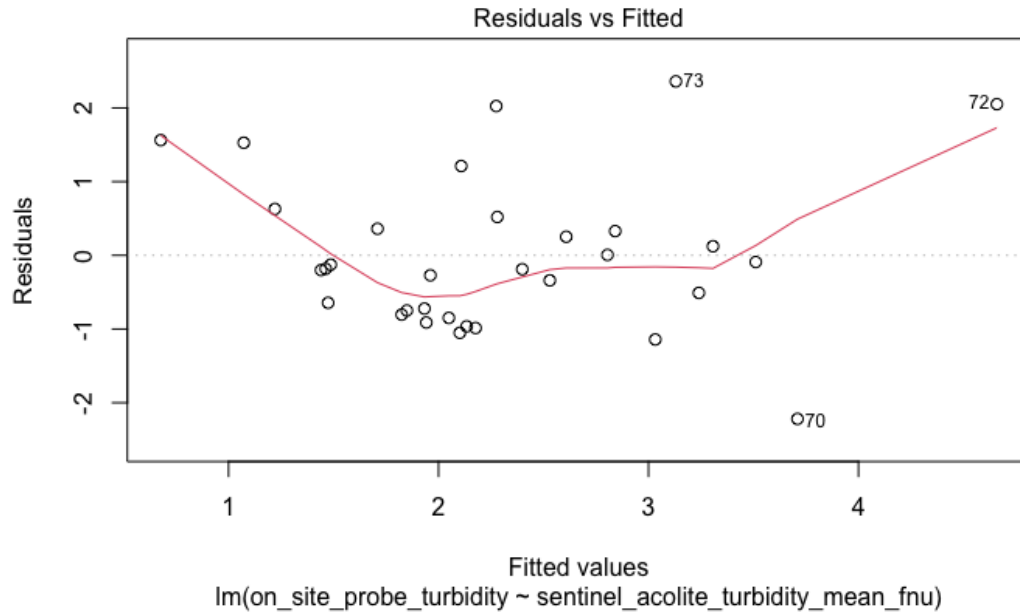


**Figure 13.** Residual vs. Fitted Plot of M1.

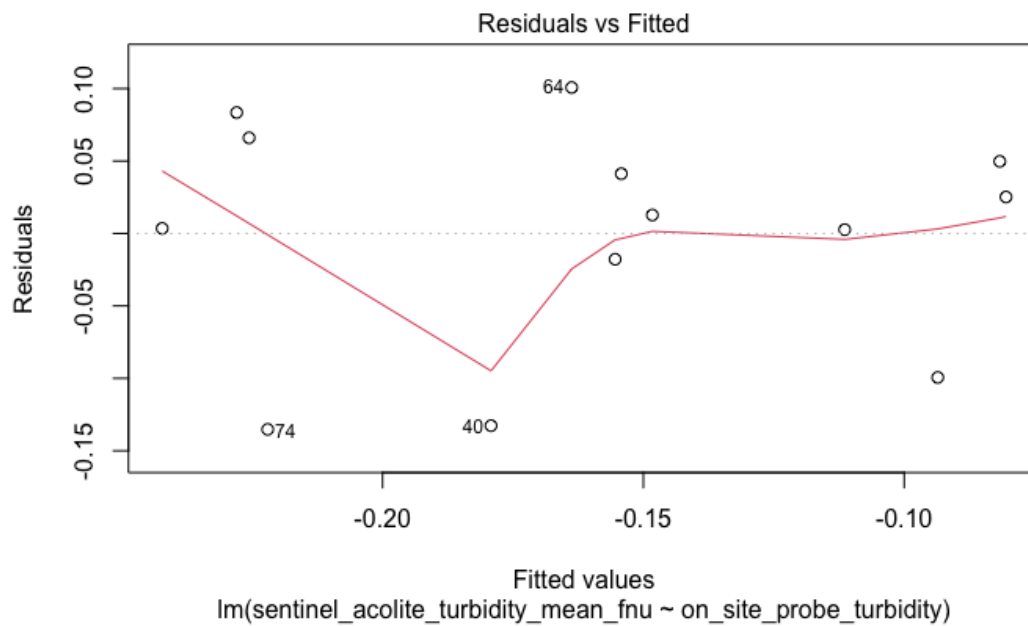


**Figure 14.** Residual vs. Fitted Plot of M2.

**8.2 - Multiple linear regression, ridge regression, and random forest for turbidity**

Overall, the ridge regression model produces the highest  $R^2$  value for predicting the on-site turbidity, which is likely due to ridge regression’s ability to prevent overfitting with small sample sizes. The importance plot from the random forest model illustrates the importance of the

ACOLITE-derived turbidity and the GEE-derived turbidity as the most important and third most important, respectively. It shows that remote sensing data is indeed helpful in explaining the variation in on-site probe turbidity in the random forest model.

All three multivariable regression models, including MLR, ridge, and random forest are more robust compared to the univariate SLR model. In all three indicators of model performance ( $R^2$  values for predicted vs. actual, MAE, and RMSE) we observed, there is improvement seen in the multivariable models. Our observation is further validated with 4-fold cross validation with 10 repeats, indicating that our multivariable models do not lead to overfitting.

### ***8.3 - Future research with Landsat***

Due to availability and weather restraints, our team ended up sampling more Sentinel-2AB than Landsat-8 overpass days. Halfway through the project, we decided to focus on Sentinel-2AB to maximize our result analysis capabilities. However, our small Landsat dataset shows great promise. We recommend that these preliminary results be expanded on by future researchers to gain a better understanding of how both Landsat and Sentinel can be used for water quality monitoring.

### ***8.4 - IDEXX vs. filter-plating method***

For measuring the total concentration of *E. coli* in the samples, there is a strong correlation between the filter-plating method and the IDEXX method. The  $R^2$  square value of 0.7825 indicates that more than 78% of the variation in the *E. coli* concentration observed by the filter-plating method can be explained by the IDEXX method. Thus, we conclude that the IDEXX method is effective at monitoring total *E. coli* concentration in the samples we collected.

Through the two linear regression models, we found that the values derived from the IDEXX method are not effective at reflecting the values derived from the filter-plating method for measuring antibiotic-resistant *E. coli*. For samples where there is antibiotic-resistant *E. coli* present, the IDEXX method tends to overestimate levels. This overestimation could be the result of high antibiotic-resistant *E. coli* concentrations not being detected in most of our samples, giving us little data and making it difficult to compare methods. Additionally, since IDEXX has not been validated as a method to measure antibiotic resistance, our methodology may also

require some modifications. Still, we conclude that there is a certain degree of association between the two methods as the  $p$ -value of the chi-square test is statistically significant.

### **8.5 - Bacterial growth mode: planktonic vs. biofilm**

One primary difference between the filter-plating and IDEXX methods for measuring FIB is the bacterial growth mode both methods allow for. Bacteria have two main forms of growth that affect their interaction with their immediate environment: planktonic and biofilm. Planktonic growth refers to bacteria floating freely in a medium (in this case, the ocean). For biofilm growth, the bacteria form a clump, generally on a surface, and grow as a collective unit. Bacteria operating under biofilm growth consistently tolerate higher levels of antibiotics than planktonically growing bacteria because of the additional protection and shelter biofilms provide (Cerca et al., 2005). In fact, biofilm bacteria can require up to 1,000 times higher concentrations of antibiotics to be effective (Ceri et al., 1999). However, it remains unclear the degree to which biofilm growth is prevented by environmental conditions like turbulent flow in marine environments (Zhang et al., 2019). In our results, we found a greater percentage of ARB using the filter-plating method, where bacteria are able to grow in biofilms on the plate media. The IDEXX method also has a limitation on the minimum bacteria levels it can detect due to the required dilution ratio. Thus, differing growth modes combined with IDEXX's detection limit are possible explanations for the difference found between the IDEXX and filter-plating methods for our ARB data collection and should be explored further.

### **8.6 - Fecal indicator bacteria vs. turbidity**

The 2019 Practicum Project led by Dr. Jennifer Jay on MRSA in Los Angeles beaches found that turbidity was significantly associated with MRSA concentrations at Venice Beach (Rugh, 2021). That project continued over the course of two years and resulted in 63 water samples collected from Venice Beach. Since our team's sampling capacity was restricted by our five-month project timeline, our satellite-derived turbidity and *in situ* water quality comparisons were limited to substantially fewer data points. The only statistically significant correlation between satellite-derived turbidity and FIB levels was found with antibiotic-resistant *E. coli* enumerated from the IDEXX method. Because the IDEXX method failed to show a strong correlation for detecting antibiotic-resistant *E. coli* with the

filter-plating method, this relationship cannot be considered conclusive. With more data collected, there is potential for a stronger relationship between satellite-derived turbidity, bacteria levels, and other water quality variables to be discovered.

### **8.7 - Spatial distribution of *E. coli***

Santa Monica had the highest concentration of *E. coli* out of all eight sampling sites along the Los Angeles coastline. The relatively high amount of tourism near the Santa Monica Pier is a likely explanation because tourism attracts more urban waste and birds, resulting in fecal pollution throughout the area. According to the City of Santa Monica, tourism attracts over eight million visitors to the city annually (City of Santa Monica, n.d.). However, very few *E. coli* at Santa Monica exhibited antibiotic resistance. The majority of antibiotic-resistant *E. coli* found in our data were from the Malibu sites, specifically Malibu 2 and 3 near the lagoon outlet. Many wetlands and lagoons naturally filter water and can reduce bacteria concentrations. However, some lagoons can have favorable conditions for bacteria growth, and they become sources of bacteria (Kawecki et al., 2017). According to a report from the City of Malibu, the Malibu Lagoon is a source of FIB like *E. coli* (Izbicki, 2011). This is likely due to upstream WWTP/urban runoff and wildlife feces. Bacteria tend to prioritize their ARGs if there are antibiotics present in their immediate environment (Zhang et al., 2016). Due to having a slow flow rate, it is possible the lagoon harbors levels of antibiotics that encourage resistance to proliferate among the bacteria present. Malibu sites 2 and 3 are impacted by effluent from the lagoon, and likely as a result, experience higher levels of *E. coli* and their antibiotic-resistant counterparts.

These findings align with Heal the Bay's Beach Report Card grades (Heal the Bay, n.d.). Heal the Bay is the leading non-profit authority on water quality along the West Coast and produces the only comprehensive analysis of coastline water quality in California. All county health departments are required to test beach water samples for indicator bacteria once a week during the peak summer season months to inform public health advisories. Using water sampling data from beach agency partners, Heal the Bay produces publicly available reports on beach health using an A-F grading system.

In its Beach Report Card annual grades, the Santa Monica Pier has historically performed very poorly. During the winter seasons between 2010-2020, the site received 10 D/F grades

(“Poor” or “Very Poor” water quality) from samples taken during dry weather. During the summer seasons between 2010-2020, the site received only slightly better results with 6 D/F grades from samples taken during dry weather. Samples taken during wet weather periods were all F grades except for 1 year that received a C. Near our Malibu 2 and 3 sampling sites, Heal the Bay’s Malibu Lagoon breach site has shown lower water quality than other Malibu sites further from the lagoon. During the winter seasons between 2010-2020, the site received 9 D/F grades from samples taken during dry weather. Samples taken during wet weather periods were all D/F grades. However, during the summer seasons between 2010-2020, the site only received 1 D/F grade from samples taken during dry weather. These results suggest that warmer weather and less stormwater runoff may be large factors in decreasing bacteria concentration in the lagoon during the summer months. Near our Malibu 1 sampling site, Heal the Bay’s “Surfrider Beach” has shown historically much cleaner water receiving mostly A and B grades between 2010-2020.

While these report cards provide the best available coastal water sample analyses, Heal the Bay recognizes the inefficiency of traditional water quality sampling and associated weekly grades for best informing the public. By the time samples have been collected and processed, a minimum of 18-24 hours have passed, and the information may be outdated. In response, Heal the Bay has created a program called NowCast that uses predictive modeling to issue daily water quality information for 25 California beaches (Heal the Bay, 2021). Computer models examine correlations between environmental conditions (e.g. temperature and tide) and historical bacteria concentrations. These correlations are used to predict how much bacteria could be present in the water given current local conditions at the beach. Local health agencies can then make more timely public notifications of unsafe water quality in the morning before most people arrive at the beach. During the summer swim season of 2017, NowCast predicted a median of 50% of the days when beach water quality failed to meet health standards. As these models develop, incorporating remote sensing data may be a way to increase accuracy and timeliness. Our team recommends combining predictive environmental modeling with satellite-derived turbidity measurements as a point of future research.

### ***8.8 - Seasonal effects***

Upwelling refers to a process in which water from deep below the ocean surface is pushed to the surface, bringing with it cooler water and increased nutrient levels (NOAA, 2021).

Along the California coast, upwelling typically occurs during the spring and summer months. Because of this overlap with our project timeline, we looked at the potential relationship between upwelling and our measured *in situ* results to maximize use of available environmental data. Our team used the Bakun Index because it had values available after March 2022 that did not require running a separate simulation. It should be noted that the Bakun Index has its limitations and the data used was for sites slightly south of our sampling sites (33N). In our results, we found that including the index as a predictor variable in the MLR model had a slight positive impact. Thus, further research should be done to look at other upwelling indices that can be used more precisely and how they relate to *in situ* and satellite water quality data.

### ***8.9 - Potential sources of error***

With 8 group members performing field sampling, lab analysis, and results analysis, our team had a wide distribution of tasks and possible variability in the execution of study methods. Additionally, because some of the methods we used are more novel and not yet fully understood, there is a steeper learning curve. In terms of lab work, the IDEXX method has some potential for error with its ability to exhibit false positives of non-target bacteria. With all of the parameters we were testing, we did not have the capacity to isolate and confirm bacteria species from IDEXX. We instead relied on validating the method with the traditional filter-plating method. In terms of remote sensing, there are some challenges with relying on satellites for continuous turbidity measurements. Many satellites have a long revisit time (e.g. Landsat-8 is on a 16-day cycle). While the satellite provides high-resolution images, a cloudy day can negate all images until the next overpass. Some satellites have a quicker revisit time, but these typically record lower resolution images unfit for turbidity measurements (Chen et al., 2007). Furthermore, many sampling dates had small clouds covering the exact coordinates of our sampling location, which would mask the turbidity reading. At times, ACOLITE coordinates had to be moved by up to 200 feet to get a viable reading. Additionally, GEE turbidity fluctuated greatly between small coordinate changes. A change in 0.0001 of the coordinate location could change the measured turbidity value by up to 4 NTU. Due to the manual GEE interface, it was difficult to achieve sufficient precision. However, we do not expect this to significantly affect our results since we are looking for overall correlation patterns rather than site-specific relationships.

## 9. CONCLUSION

This report provides 5 months of data collection on the viability of using remote sensing and the IDEXX method as proxies for coastal water quality analysis. In summary, the main findings were:

- The simple linear regression model for satellite-derived turbidity vs. on-site turbidity was inconsistent. However, the model's robustness improved when outliers were removed and a clustering analysis was applied.
- Among three multivariable models, ridge regression had the best performance, likely due to its advantage when dealing with small data sets.
- No correlations between satellite-derived turbidity and FIB levels were found in our data.
- The IDEXX method is effective at monitoring total *E. coli* concentration, but not the percentage of antibiotic-resistant *E. coli*.
- The majority of total *E. coli* was found in Santa Monica, but sites near the Malibu Lagoon exhibited the highest percentage of antibiotic-resistant *E. coli*

These findings highlight the potential to greatly improve water quality monitoring with the eventual inclusion of both *in situ*- and satellite-acquired data into algorithms used for recreational beaches. However, more research is needed to further inform and build on our findings. As a resource, this report should be provided to NASA's Jet Propulsion Laboratory, the National Oceanic and Atmospheric Administration, Heal the Bay, and any other entities interested in monitoring coastal waters in Southern California.

## 10. ACKNOWLEDGEMENTS

We would like to thank the many friends, family, and mentors who have made this project possible. Thank you to Yuwei Kong and Karina Jimenez for diligently overseeing and supporting our lab work and weekly progress. Thank you to Dr. Jennifer Jay for your neverending enthusiasm and encouragement, and thank you to both Dr. Jennifer Jay and Dr. Christine Lee for devising the structure of this project. Thank you to Scott Gruber for your help in designing a

website for our project. Lastly, thank you to Noah Garrison for leading the Environmental Science Practicum Program and allowing us to gain this invaluable hands-on experience.

## 11. REFERENCES

- Akiyama, T., & Savin, M. C. (2010). Populations of antibiotic-resistant coliform bacteria change rapidly in a wastewater effluent dominated stream. *Science of The Total Environment*, 408(24), 6192–6201. <https://doi.org/10.1016/j.scitotenv.2010.08.055>
- Amarasiri, M., Sano, D., & Suzuki, S. (2019). Understanding human health risks caused by antibiotic resistant bacteria (ARB) and antibiotic resistance genes (ARG) in water environments: Current knowledge and questions to be answered. *Critical Reviews in Environmental Science and Technology*, 50(19), 2016-2059. <https://doi.org/10.1080/10643389.2019.1692611>
- Aram, S. A., Saalidong, B. M., & Lartey, P. O. (2021). Comparative assessment of the relationship between coliform bacteria and water geochemistry in surface and ground water systems. *PLOS ONE*, 16(9), e0257715. <https://doi.org/10.1371/journal.pone.0257715>
- Baquero, F., Martínez, J.-L., & Cantón, R. (2008). Antibiotics and antibiotic resistance in water environments. *Current Opinion in Biotechnology*, 19(3), 260–265. <https://doi.org/10.1016/j.copbio.2008.05.006>
- Barrell, R. A.E., Cole, S. R., Down, R., Fricker, C., Holmes, P., Jones, C., Lightfoot, N., Sartory, D., Scanlon, S., Taylor, J. A., Tillet, H. E. and Watkins, J. (1997). Evaluation Trials for Two Media for the Simultaneous Detection and Enumeration of *Escherichia coli* and coliform organisms. *Methods for the Examination of Waters and Associated Materials* UK Environment Agency.
- Beach Report Card*. Heal the Bay. (n.d.). Retrieved 2022, from <https://beachreportcard.org/33.910299999999999/-118.51929100000001/11>
- Beaches Environmental Assessment and Coastal Health (BEACH) Act, 33 U.S.C. § 1313 *et seq.* (2000). <https://www.congress.gov/106/plaws/publ284/PLAW-106publ284.pdf>
- Berendonk, T. U., Manaia, C. M., Merlin, C., Fatta-Kassinos, D., Cytryn, E., Walsh, F., Bürgmann, H., Sørum, H., Norström, M., Pons, M.-N., Kreuzinger, N., Huovinen, P., Stefani, S., Schwartz, T., Kisand, V., Baquero, F., & Martinez, J. L. (2015). Tackling antibiotic resistance: The environmental framework. *Nature Reviews Microbiology*, 13(5), 310–317. <https://doi.org/10.1038/nrmicro3439>

- Bonanse, M., Ledesma, M., Bazán, R., Ferral, A., German, A., O'Mill, P., Rodriguez, C., & Pinotti, L. (2019). Evaluating the feasibility of using Sentinel-2 imagery for water clarity assessment in a reservoir. *Journal of South American Earth Sciences*, *95*, 102265.  
<https://doi.org/10.1016/j.jsames.2019.102265>
- Budnick, G. E., Howard, R. T., & Mayo, D. R. (1996). Evaluation of enterolert for enumeration of enterococci in recreational waters. *Applied and Environmental Microbiology*, *62*(10), 3881–3884. <https://doi.org/10.1128/aem.62.10.3881-3884.1996>
- Centers for Disease Control and Prevention (CDC). (2019). *Parasites - cryptosporidium (also known as "crypto")*. U.S. Department of Health and Human Services.  
<https://www.cdc.gov/parasites/crypto/index.html>
- Centers for Disease Control and Prevention (CDC). (2020). *How Antibiotic Resistance Happens*. U.S. Department of Health & Human Services.  
<https://www.cdc.gov/drugresistance/about/how-resistance-happens.html>
- Centers for Disease Control and Prevention (CDC). (2021). *About Antibiotic Resistance*. U.S. Department of Health & Human Services. <https://www.cdc.gov/drugresistance/about.html>
- Cerca, N., Martins, S., Cerca, F., Jefferson, K. K., Pier, G. B., Oliveira, R., & Azeredo, J. (2005). Comparative assessment of antibiotic susceptibility of coagulase-negative staphylococci in biofilm versus planktonic culture as assessed by bacterial enumeration or rapid XTT colorimetry. *Journal of Antimicrobial Chemotherapy*, *56*(2), 331–336.  
<https://doi.org/10.1093/jac/dki217>
- Ceri, H., Olson, M. E., Stremick, C., Read, R. R., Morck, D., & Buret, A. (1999). The Calgary biofilm device: New technology for rapid determination of antibiotic susceptibilities of bacterial biofilms. *Journal of Clinical Microbiology*, *37*(6), 1771–1776.  
<https://doi.org/10.1128/JCM.37.6.1771-1776.1999>
- Chen, Z., Hu, C., & Muller-Karger, F. (2007). Monitoring turbidity in Tampa Bay using MODIS/Aqua 250-m imagery. *Remote Sensing of Environment*, *109*(2), 207–220.  
<https://doi.org/10.1016/j.rse.2006.12.019>
- City of Santa Monica. (n.d.). *About Us*. Home Page. Retrieved 2022, from  
<https://www.santamonica.gov/about>
- Cleveland Water Department. (2019). *Understanding Turbidity and Why it Matters*.  
<https://www.clevelandwater.com/blog/understanding-turbidity-and-why-it-matters>

- Cogliani, C., Goossens, H., & Greko, C. (2011). Restricting antimicrobial use in food animals: Lessons from Europe. *Microbe Magazine*, 6(6), 274–279.  
<https://doi.org/10.1128/microbe.6.274.1>
- Collignon, P. (2009). Resistant *Escherichia coli*—we are what we eat. *Clinical Infectious Diseases*, 49(2), 202–204. <https://doi.org/10.1086/599831>
- Coman, Cristian. (2016). Antibiotic resistance: not only the clinician's problem. *Danube News*. 18. 2-5.
- Diamant, S. (2013). The importance of monitoring turbidity in industrial water treatment. *Water Technology Online*. <https://www.watertechnology.com/wastewater/article/15543707/the-importance-of-monitoring-turbidity-in-industrial-water-treatment>
- Eckner, K. F. (1998). Comparison of membrane filtration and multiple-tube fermentation by the COLILERT and Enterolert methods for detection of waterborne coliform bacteria, *Escherichia coli*, and enterococci used in drinking and bathing water quality monitoring in southern Sweden. *Applied and Environmental Microbiology*, 64(8), 3079–3083.  
<https://doi.org/10.1128/aem.64.8.3079-3083.1998>
- Economou, V., & Gousia, P. (2015). Agriculture and food animals as a source of antimicrobial-resistant bacteria. *Infection and Drug Resistance*, 8, 49–61.  
<https://doi.org/10.2147/IDR.S55778>
- Edberg, S. C., Allen, M. J., Smith, D. B., & Kriz, N. J. (1990). Enumeration of total coliforms and *Escherichia coli* from source water by the defined substrate technology. *Applied and Environmental Microbiology*, 56(2), 366–369.  
<https://doi.org/10.1128/aem.56.2.366-369.1990>
- Edberg, S. C., Allen, M. J., & Smith, D. B. (1991). Defined substrate technology method for rapid and specific simultaneous enumeration of total coliforms and *Escherichia coli* from water: Collaborative Study. *Journal of AOAC INTERNATIONAL*, 74(3), 526–529.  
<https://doi.org/10.1093/jaoac/74.3.526>
- European Space Agency (ESA). (n.d.a). Copernicus: Europe's eyes on Earth. *About Copernicus*.  
<https://www.copernicus.eu/en/about-copernicus>
- European Space Agency (ESA). (n.d.b). Sentinel Online. *Satellite Description*.  
<https://sentinels.copernicus.eu/web/sentinel/missions/sentinel-2/satellite-description>
- Ferguson, D. M., Griffith, J. F., McGee, C. D., Weisberg, S. B., & Hagedorn, C. (2013).

- Comparison of Enterococcus Species Diversity in Marine Water and Wastewater Using Enterolert and EPA Method 1600. *Journal of Environmental and Public Health*, 2013, e848049. <https://doi.org/10.1155/2013/848049>
- Fricker, C. R., Fricker, E. J., Goodall, T., & Cowburn, J. (1995). Quantitative Procedures for the Detection of *E. coli*, Coliforms, and Enterococci in Water, Using Quantitray and Enterolert. In *Water Quality Technology Conference, New Orleans*.
- Fricker, E. J., & Fricker, C. R. (1996). Use of defined substrate technology and a novel procedure for estimating the numbers of Enterococci in water. *Journal of Microbiological Methods*, 27(2-3), 207–210. [https://doi.org/10.1016/s0167-7012\(96\)00950-5](https://doi.org/10.1016/s0167-7012(96)00950-5)
- Fuentes, M. D., Gutierrez, S., Sahagun, D., Gomez, J., Mendoza, J., Ellis, C. C., Bauer, S., Blattner, J., Lee, W.-Y., Alvarez, M., & Domínguez, D. C. (2019). Assessment of Antibiotic Levels, Multi-Drug Resistant Bacteria and Genetic Biomarkers in the Waters of the Rio Grande River Between the United States-Mexico Border. *Journal of Health and Pollution*, 9(23), 190912. <https://doi.org/10.5696/2156-9614-9.23.190912>
- Galvin, S., Boyle, F., Hickey, P., Vellinga, A., Morris, D., & Cormican, M. (2010). Enumeration and Characterization of Antimicrobial-Resistant *Escherichia coli* Bacteria in Effluent from Municipal, Hospital, and Secondary Treatment Facility Sources. *Applied and Environmental Microbiology*, 76(14), 4772–4779. <https://doi.org/10.1128/AEM.02898-09>
- Graham, C. (1999). Comparison of Coliform/*Escherichia coli* Count Methods Trial. *UK Public Health Laboratory System, Water & Environmental Research Unit (Nottingham)*.
- Greenberg, A. E., Clesceri, L. S., Eaton, A. D., & Franson, M. A. H. (1992). *Standard methods for the examination of water and wastewater* (18th ed). American public health Association (APHA). <https://law.resource.org/pub/us/cfr/ibr/002/apha.method.9221.1992.pdf>
- Gonzales, H. B., Ravi, S., Li, J., & Sankey, J. B. (2018). Ecohydrological implications of aeolian sediment trapping by sparse vegetation in drylands. *Ecohydrology*, 11(7), e1986. <https://doi.org/10.1002/eco.1986>
- Griffin, D. W., Banks, K., Gregg, K., Shedler, S., & Walker, B. K. (2020). Antibiotic Resistance in Marine Microbial Communities Proximal to a Florida Sewage Outfall System. *Antibiotics*, 9(3), 118. <https://doi.org/10.3390/antibiotics9030118>

- Hannouche, A., Ghassan, C., Ruban, G., Tassin, B., Bruno, J., Lemaire, B. J., Joannis, C. (2011). Relationship between turbidity and total suspended solids concentration within a combined sewer system. *National Center for Biotechnology Information*.  
<https://pubmed.ncbi.nlm.nih.gov/22170840/>
- Hollis, A., & Ahmed, Z. (2013). Preserving Antibiotics, Rationally. *New England Journal of Medicine*, 369(26), 2474–2476. <https://doi.org/10.1056/NEJMp1311479>
- Huycke, M. M., Sahm, D. F., & Gilmore, M. S. (1998). Multiple-drug resistant enterococci: the nature of the problem and an agenda for the future. *Emerging infectious diseases*, 4(2), 239.
- Irvine, K., Somogyi, E., & Pettibone, G. (2002). Turbidity, suspended solids, and bacteria relationships in the Buffalo River Watershed. *Middle States Geographer*, 35.
- Izbicki, J. (2011). *Distribution of Fecal Indicator Bacteria along the Malibu, California, Coastline* (USGS Numbered Series No. 2011–1091; Open-File Report, pp. 1–8). United States Geological Survey (USGS). U.S. Department of the Interior  
<https://www.malibucity.org/DocumentCenter/View/923/Distribution-of-Fecal-Indicator-Bacteria-along-the-Malibu-California-Coastline>
- Jain, S., & Marothi, Y. (2014). A Study of Antimicrobial Resistance in Clinical Isolates of Enterococci. *National Journal of Integrated Research in Medicine*, 5(6).
- Kawecki, S., Kuleck, G., Dorsey, J. H., Leary, C., & Lum, M. (2017). The prevalence of antibiotic-resistant bacteria (ARB) in waters of the Lower Ballona Creek Watershed, Los Angeles County, California. *Environmental Monitoring and Assessment*, 189(6), 261.  
<https://doi.org/10.1007/s10661-017-5964-9>
- Khardori, N. M. (2012). In-feed antibiotic effects on the swine intestinal microbiome. *Yearbook of Medicine*, 2012, 61–63. <https://doi.org/10.1016/j.ymed.2012.08.009>
- Kim, D.-W., & Cha, C.-J. (2021). Antibiotic resistome from the one-health perspective: Understanding and controlling antimicrobial resistance transmission. *Experimental & Molecular Medicine*, 53(3), 301–309. <https://doi.org/10.1038/s12276-021-00569-z>
- Kinzelman, J. L., Singh, A., Ng, C., Pond, K. R., Bagley, R. C., & Gradus, S. (2005). Use of idexx colilert-18® and Quanti-Tray/2000 as a rapid and simple enumeration method for the implementation of Recreational Water Monitoring and notification programs. *Lake and Reservoir Management*, 21(1), 73–77. <https://doi.org/10.1080/07438140509354414>

- Le, T., Ng, C., Tran, N. H., Chen, H., & Gin, K. Y. (2018). Removal of antibiotic residues, antibiotic resistant bacteria and antibiotic resistance genes in municipal wastewater by membrane bioreactor systems. *Water Research, 145*, 498-508.  
<https://doi.org/10.1016/j.watres.2018.08.060>
- Lim, J., & Choi, M. (2015). Assessment of water quality based on Landsat 8 operational land imager associated with human activities in Korea. *Environmental Monitoring and Assessment, 187*(6), 384. <https://doi.org/10.1007/s10661-015-4616-1>
- Mallin, M., Johnson, V., & Ensign, S. (2009). Comparative Impacts of Stormwater Runoff on Water Quality of an Urban, a Suburban, and a Rural Stream. *Environmental Monitoring and Assessment, 159*, 475–491. <https://doi.org/10.1007/s10661-008-0644-4>
- Manyi-Loh, C., Mamphweli, S., Meyer, E., & Okoh, A. (2018). Antibiotic use in agriculture and its consequential resistance in environmental sources: Potential Public Health Implications. *Molecules, 23*(4), 795. <https://doi.org/10.3390/molecules23040795>
- McLain, J. E., Cytryn, E., Durso, L. M., & Young, S. (2016). Culture-based Methods for Detection of Antibiotic Resistance in Agroecosystems: Advantages, Challenges, and Gaps in Knowledge. *Journal of Environmental Quality, 45*(2), 432–440.  
<https://doi.org/10.2134/jeq2015.06.0317>
- Murray, K. S., Fisher, L. E., Therrien, J., George, B., & Gillespie, J. (2001). Assessment and Use of Indicator Bacteria to Determine Sources of Pollution to an Urban River. *Journal of Great Lakes Research, 27*(2), 220–229. [https://doi.org/10.1016/S0380-1330\(01\)70635-1](https://doi.org/10.1016/S0380-1330(01)70635-1)
- NASA. (n.d.). *Landsat 8*. U.S. Department of the Interior.  
<https://landsat.gsfc.nasa.gov/landsat-8/landsat-8-overview>
- Nnadozie, C. F., & Odume, O. N. (2019). Freshwater environments as reservoirs of antibiotic resistant bacteria and their role in the dissemination of antibiotic resistance genes. *Environmental Pollution, 254*, 113067. <https://doi.org/10.1016/j.envpol.2019.113067>
- NOAA. (2020). *Ocean acidification*. U.S. Department of the Interior.  
<https://www.noaa.gov/education/resource-collections/ocean-coasts/ocean-acidification>
- NOAA. (2021) *What is upwelling?* Retrieved May 31, 2022, from  
<https://oceanservice.noaa.gov/facts/upwelling.html>
- NOAA Great Lakes Environmental Research Laboratory (GLERL), (n.d.). *Fecal Indicator Bacteria Monitoring*. National Oceanic and Atmospheric Administration (NOAA). U.S.

- Department of Commerce.  
[https://www.glerl.noaa.gov/res/HABs\\_and\\_Hypoxia/nearshoreFIB/index.html](https://www.glerl.noaa.gov/res/HABs_and_Hypoxia/nearshoreFIB/index.html)  
*Nowcast Daily Beach water quality predictions now online*. Heal the Bay. (2021, June 1).  
Retrieved from  
<https://healthebay.org/nowcast-daily-beach-water-quality-predictions-2021/>
- Operators Unlimited. (2021). Turbidity in Industrial Wastewater: What is it and Why Measure?  
Operators Unlimited.  
<https://www.operatorsunlimited.net/turbidity-in-industrial-wastewater-what-is-it-and-why-measure/>
- Overbey, K. N., Hatcher, S. M., & Stewart, J. R. (2015). Water quality and antibiotic resistance at beaches of the Galápagos Islands. *Frontiers in Environmental Science*, 3.  
<https://www.frontiersin.org/article/10.3389/fenvs.2015.00064>
- Peperzak, L., & van Bleijswijk, J. (2021). False-positive enterococci counts in seawater with the IDEXX Enterolert-E most probable number technique caused by *Bacillus licheniformis*. *Environmental Science and Pollution Research*, 28(9), 10654–10660.  
<https://doi.org/10.1007/s11356-020-11342-6>
- Pisciotta, J. M., Rath, D. F., Stanek, P. A., Flanery, D. M., & Harwood, V. J. (2002). Marine Bacteria Cause False-Positive Results in the Colilert-18 Rapid Identification Test for *Escherichia coli* in Florida Waters. *Applied and Environmental Microbiology*, 68(2), 539–544. <https://doi.org/10.1128/AEM.68.2.539-544.2002>
- Ramoutar, S. (2020). The use of Colilert-18, Colilert and Enterolert for the detection of faecal coliform, *Escherichia coli* and Enterococci in tropical marine waters, Trinidad and Tobago. *Regional Studies in Marine Science*, 40.  
<https://doi.org/10.1016/j.rsma.2020.101490>
- Rawat, D., & Nair, D. (2010). Extended-spectrum  $\beta$ -lactamases in gram negative bacteria. *Journal of Global Infectious Diseases*, 2(3), 263.  
<https://doi.org/10.4103/0974-777X.68531>
- Reinthaler, F. F., Posch, J., Feierl, G., Wüst, G., Haas, D., Ruckebauer, G., Mascher, F., & Marth, E. (2003). Antibiotic resistance of *E. coli* in sewage and sludge. *Water Research*, 37(8), 1685–1690. [https://doi.org/10.1016/s0043-1354\(02\)00569-9](https://doi.org/10.1016/s0043-1354(02)00569-9)
- Rice, E. W., Allen, M. J., & Edberg, S. C. (1990). Efficacy of beta-glucuronidase assay for

- identification of escherichia coli by the defined-substrate technology. *Applied and Environmental Microbiology*, 56(5), 1203–1205.  
<https://doi.org/10.1128/aem.56.5.1203-1205.1990>
- Roe, M., & Pillai, S. (2003). Monitoring and identifying antibiotic resistance mechanisms in bacteria. *Poultry Science*, 82(4), 622–626. <https://doi.org/10.1093/ps/82.4.622>
- Rompré, A., Servais, P., Baudart, J., de-Roubin, M.-R., & Laurent, P. (2002). Detection and enumeration of coliforms in drinking water: Current methods and emerging approaches. *Journal of Microbiological Methods*, 49(1), 31–54.  
[https://doi.org/10.1016/s0167-7012\(01\)00351-7](https://doi.org/10.1016/s0167-7012(01)00351-7)
- Roy, D. P., Wulder, M. A., Loveland, T. R., C.E., W., Allen, R. G., Anderson, M. C., Helder, D., Irons, J. R., Johnson, D. M., Kennedy, R., Scambos, T. A., Schaaf, C. B., Schott, J. R., Sheng, Y., Vermote, E. F., Belward, A. S., Bindschadler, R., Cohen, W. B., Gao, F., ... Zhu, Z. (2014). Landsat-8: Science and product vision for terrestrial global change research. *Remote Sensing of Environment*, 145, 154–172.  
<https://doi.org/10.1016/j.rse.2014.02.001>
- Rugh, M. B. (2021). Methicillin-resistant Staphylococcus aureus in Southern California coastal waters: environmental exposure to humans and stormwater biofilters as a preventative solution. *UCLA*. ProQuest ID: Rugh\_ucla\_0031D\_19562. Merritt ID: ark:/13030/m5kx16cr. Retrieved from <https://escholarship.org/uc/item/11b3q62w>
- Schulte to Bühne, H., & Pettorelli, N. (2018). Better together: Integrating and fusing multispectral and radar satellite imagery to inform biodiversity monitoring, ecological research and conservation science. *Methods in Ecology and Evolution*, 9(4), 849–865.  
<https://doi.org/10.1111/2041-210X.12942>
- Sent, G., Biguino, B., Favareto, L., Cruz, J., Sá, C., Dogliotti, A. I., Palma, C., Brotas, V., & Brito, A. C. (2021). Deriving Water Quality Parameters Using Sentinel-2 Imagery: A Case Study in the Sado Estuary, Portugal. *Remote Sensing*, 13(5), 1043.  
<https://doi.org/10.3390/rs13051043>
- Sercu, B., Van De Werfhorst, L. C., Murray, J. L. S., & Holden, P. A. (2011). Cultivation-Independent Analysis of Bacteria in IDEXX Quanti-Tray/2000 Fecal Indicator Assays. *Applied and Environmental Microbiology*, 77(2), 627–633.  
<https://doi.org/10.1128/AEM.01113-10>

- Shanthi, M., & Sekar, U. (2010). Extended spectrum beta lactamase producing *Escherichia coli* and *Klebsiella pneumoniae*: risk factors for infection and impact of resistance on outcomes. *J Assoc Physicians India*, 58(Suppl), 41-44.
- Stalder, T., Press, M. O., Sullivan, S., Liachko, I., & Top, E. M. (2019). Linking the resistome and plasmidome to the microbiome. *The ISME Journal*, 13(10), 2437–2446.  
<https://doi.org/10.1038/s41396-019-0446-4>
- Thackston, E. L., and Palermo, M. R. (2000). Improved methods for correlating turbidity and suspended solids for monitoring. *DOER Technical Notes Collection*. <https://www.wes.army.mil/el/dots/doer>
- Toming, K., Kutser, T., Laas, A., Sepp, M., Paavel, B., & Nõges, T. (2016). First Experiences in Mapping Lake Water Quality Parameters with Sentinel-2 MSI Imagery. *Remote Sensing*, 8(8), 640. <https://doi.org/10.3390/rs8080640>
- U.S. Environmental Protection Agency (EPA). (n.d.a). *5.7 Nitrates*. Water: Monitoring and Assessment. U.S. Department of the Interior.  
<https://archive.epa.gov/water/archive/web/html/vms57.html>
- U.S. Environmental Protection Agency (EPA). (n.d.b). *5.8 Total Solids*. Water: Monitoring and Assessment. U.S. Department of the Interior.  
<https://archive.epa.gov/water/archive/web/html/vms58.html>
- U.S. Environmental Protection Agency (EPA). (n.d.c). *5.11 Fecal Bacteria*. Water: Monitoring and Assessment. U.S. Department of the Interior.  
<https://archive.epa.gov/water/archive/web/html/vms511.html>
- U.S. Environmental Protection Agency (EPA). (2003). Guidelines Establishing Test Procedures for the Analysis of Pollutants; Analytical Methods for Biological Pollutants in Ambient Water; Final Rule.
- U.S. Environmental Protection Agency (EPA). (2013a). *Indicators: Conductivity*. National Aquatic Resource Surveys. [Overviews and Factsheets]. U.S. Department of the Interior.  
<https://www.epa.gov/national-aquatic-resource-surveys/indicators-conductivity>
- U.S. Environmental Protection Agency (EPA). (2013b). *Indicators: Phosphorus*. National Aquatic Resource Surveys. [Overviews and Factsheets]. U.S. Department of the Interior.  
<https://www.epa.gov/national-aquatic-resource-surveys/indicators-phosphorus>
- USGS Earth Resources Observation and Science (EROS) Center. (2019). *Comparison of*

- Sentinel-2 and Landsat*. United States Geological Survey (USGS). U.S. Department of the Interior.  
[https://www.usgs.gov/centers/eros/science/usgs-eros-archive-sentinel-2-comparison-sentinel-2-and-landsat?qt-science\\_center\\_objects=0#qt-science\\_center\\_objects](https://www.usgs.gov/centers/eros/science/usgs-eros-archive-sentinel-2-comparison-sentinel-2-and-landsat?qt-science_center_objects=0#qt-science_center_objects)
- USGS Water Science School. (2018a). *Dissolved Oxygen and Water*. United States Geological Survey (USGS). U.S. Department of the Interior.  
<https://www.usgs.gov/special-topics/water-science-school/science/dissolved-oxygen-and-water>
- USGS Water Science School. (2018b). *Turbidity and Water*. United States Geological Survey (USGS). U.S. Department of the Interior.  
<https://www.usgs.gov/special-topics/water-science-school/science/turbidity-and-water>
- USGS Water Science School. (2019). *pH and Water*. United States Geological Survey (USGS). U.S. Department of the Interior.  
[https://www.usgs.gov/special-topic/water-science-school/science/wastewater-treatment-water-use?qt-science\\_center\\_objects=0#qt-science\\_center\\_objects](https://www.usgs.gov/special-topic/water-science-school/science/wastewater-treatment-water-use?qt-science_center_objects=0#qt-science_center_objects)
- United States Naval Academy (USNA). (2021). *Landsat versus Sentinel-2 Comparison*.  
[https://www.usna.edu/Users/oceano/pguth/md\\_help/remote\\_sensing\\_course/landsat\\_sentinel2.html](https://www.usna.edu/Users/oceano/pguth/md_help/remote_sensing_course/landsat_sentinel2.html)
- Vail, J. H., Morgan, R., Merino, C. R., Gonzales, F., Miller, R., & Ram, J. L. (2003). Enumeration of waterborne escherichia coli with PETRIFILM plates. *Journal of Environmental Quality*, 32(1), 368–373. <https://doi.org/10.2134/jeq2003.3680>
- Vikesland, P. J., Pruden, A., Alvarez, P. J. J., Aga, D., Bürgmann, H., Li, X., Manaia, C. M., Nambi, I., Wigginton, K., Zhang, T., & Zhu, Y.-G. (2017). Toward a Comprehensive Strategy to Mitigate Dissemination of Environmental Sources of Antibiotic Resistance. *Environmental Science & Technology*, 51(22), 13061–13066
- Wang, J., Chu, L., Wojnárovits, L., & Takács, E. (2020). Occurrence and fate of antibiotics, antibiotic resistant genes (ARGs) and antibiotic resistant bacteria (ARB) in municipal wastewater treatment plant: An overview. *Science of The Total Environment*, 744, 140997. <https://doi.org/10.1016/j.scitotenv.2020.140997>
- Wang, Y., Xia, H., Fu, J., & Sheng, G. (2004). Water quality change in reservoirs of Shenzhen, China: Detection using LANDSAT/TM data. *Science of The Total Environment*,

- 328(1–3), 195–206. <https://doi.org/10.1016/j.scitotenv.2004.02.020>
- Watts, J., Schreier, H., Lanska, L., & Hale, M. (2017). The Rising Tide of Antimicrobial Resistance in Aquaculture: Sources, Sinks and Solutions. *Marine Drugs*, 15(6), 158. <https://doi.org/10.3390/md15060158>
- World Health Assembly, 69. (2016). *Global action plan on antimicrobial resistance: Options for establishing a global development and stewardship framework to support the development, control, distribution and appropriate use of new antimicrobial medicines, diagnostic tools, vaccines and other interventions: report by the Secretariat*. World Health Organization. <https://apps.who.int/iris/handle/10665/252682>
- Wormell, P., & Rodger, A. (2013). Absorbance Spectroscopy: Overview. In G. C. K. Roberts (Ed.), *Encyclopedia of Biophysics* (pp. 23–25). Springer Berlin Heidelberg. [https://doi.org/10.1007/978-3-642-16712-6\\_784](https://doi.org/10.1007/978-3-642-16712-6_784)
- Wu, J., Su, Y., Deng, Y., Guo, Z., Mao, C., Liu, G., . . . Feng, J. (2019). Prevalence and distribution of antibiotic resistance in marine fish farming areas in Hainan, China. *Science of The Total Environment*, 653, 605-611. <https://doi.org/10.1016/j.scitotenv.2018.10.251>
- Wuijts, S., van den Berg, H. H. J. L., Miller, J., Abebe, L., Sobsey, M., Andreumont, A., Medlicott, K. O., van Passel, M.W. J., & de Roda Husman, A. M. (2017). Towards a research agenda for water, sanitation and antimicrobial resistance. *Journal of Water and Health*, 15(2), 175–184. <https://doi.org/10.2166/wh.2017.124>
- Xi, C., Zhang, Y., Marrs, C. F., Ye, W., Simon, C., Foxman, B., & Nriagu, J. (2009). Prevalence of antibiotic resistance in drinking water treatment and distribution systems. *Applied and Environmental Microbiology*, 75(17), 5714–5718. <https://doi.org/10.1128/aem.00382-09>
- Xu, L., Ouyang, W., Qian, Y., Su, C., Su, J., & Chen, H. (2016). High-throughput profiling of antibiotic resistance genes in drinking water treatment plants and distribution systems. *Environmental Pollution*, 213, 119-126. <https://doi.org/10.1016/j.envpol.2016.02.013e>
- Zhang, S., Pang, S., Wang, P., Wang, C., Han, N., Liu, B., Han, B., Li, Y., & Anim-Larbi, K. (2016). Antibiotic concentration and antibiotic-resistant bacteria in two shallow urban lakes after stormwater event. *Environmental Science and Pollution Research*, 23(10), 9984–9992. <https://doi.org/10.1007/s11356-016-6237-9>

Zhang, W., Ding, W., Li, Y.-X., Tam, C., Bougouffa, S., Wang, R., Pei, B., Chiang, H., Leung, P., Lu, Y., Sun, J., Fu, H., Bajic, V. B., Liu, H., Webster, N. S., & Qian, P.-Y. (2019). Marine biofilms constitute a bank of hidden microbial diversity and functional potential. *Nature Communications*, 10(1), 517. <https://doi.org/10.1038/s41467-019-08463-z>

# Turbidity Measurement Procedure

An accurate turbidity measurement depends on good measurement techniques. Factors such as clean sample vials, positioning of vial in the sample well, covering the vial with the light shield cover (if needed), meter calibration, handling of meter and others have to be taken into consideration. Refer to the **Vials – Handling, Cleaning and Care** and **Appendix 2 Guide to Good Measurement Technique** sections for more information.

## Preparation of Sample Vial

1. Obtain a clean and dry sample vial. See **Figure 9**. Take care to handle the sample vial by the top cap.
2. Rinse the vial with approximately 10 mL of the sample water, capping the vial with the black screw cap and gently inverting it several times. Discard the used sample and repeat the rinsing procedure two times.
4. Fill the rinsed vial with the remaining portion (approximately 10 mL) of the grab sample up to the mark indicated in the vial. Cap the vial with the supplied black screw cap.
5. Wipe the vial with the soft, lint-free cloth supplied. Ensure that the outside of the vial is dry, clean and free from smudges.
6. Apply a thin film of silicone oil (supplied) on the sample vial. See **Figure 10**.
7. Wipe the vial with a soft cloth to obtain an even distribution over the entire vial surface. The purpose of oiling the vial is to fill small scratches and to mask the imperfection in the glass. Do not apply large quantity of oil as this may collect dirt and dust.
8. The sample vial is now ready to be inserted into the sample well of the meter for measurement.

**Figure 9**  
Sample Vial

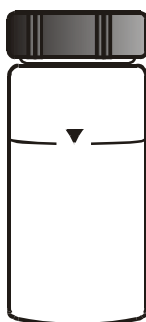
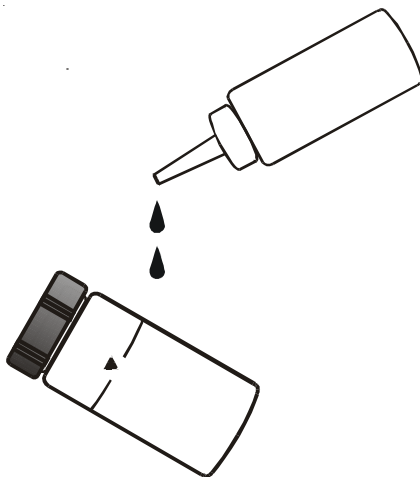


**Figure 10**  
Applying the Silicon Oil



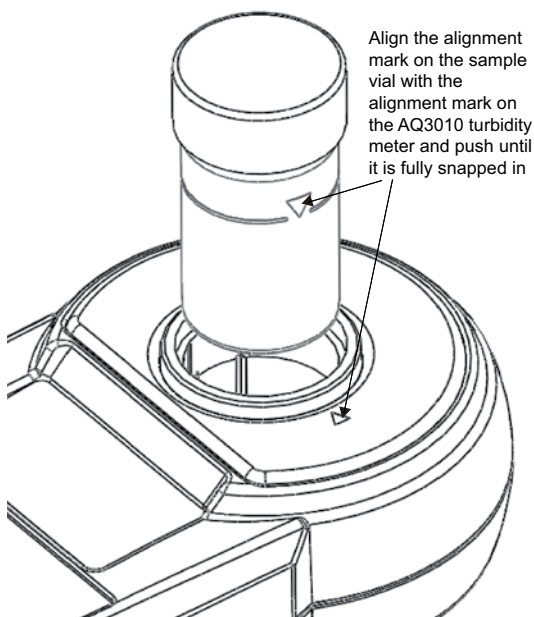
## Measurement Procedure

1. Place the AQ3010 turbidity meter on a flat and level surface.

**Note:** Do not hold the meter in your hand while operating it, as this may cause inaccurate measurements.

2. Place the sample vial inside the sample well and align the vial's alignment mark with the meter's alignment mark. See **Figure 11**.

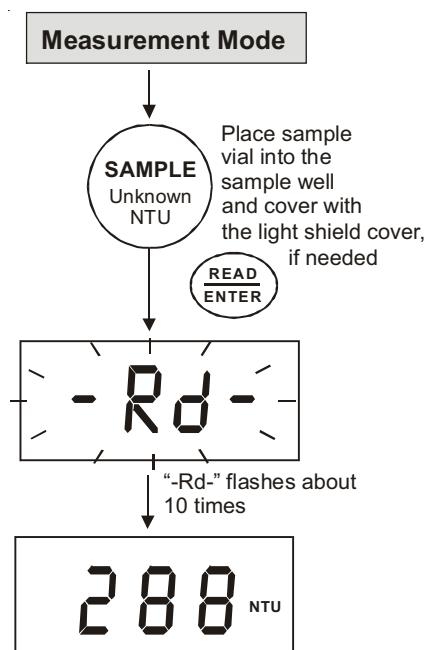
**Figure 11**  
Aligning the Sample Vial Alignment Mark with the Meter Alignment Mark



3. Push the vial down until it slides fully in.
4. Cover the vial using the light shield cover, if necessary. For many environments this is not required. The vial cap seals the sample well.
5. Turn on the meter by pressing the **ON/OFF** key.

- After the power-up sequence, the meter will go to the measurement mode and the display will blink “-Rd-” about ten times. See **Figure 12**.

**Figure 12**  
Reading a  
Turbidity Value



- The measured reading will appear in the display.
- If necessary, place the second sample vial into the sample well. Align the vial alignment mark with the meter alignment mark.
- Press the **READ/ENTER** key. The display will blink “-Rd-” several times and measured reading will appear.
- Repeat this procedure for all of your samples.

### Measurement Notes

- Never pour liquid directly into the sample well of the instrument.** Always use a 25 mm vial. The instrument will only accurately measure the turbidity of a sample when 25 mm vials sealed with the black caps are used. The black cap serves to both seal the vial and block stray light.
- Never attempt to clean the sample well. The optics may be damaged.
- For battery conservation, the instrument automatically powers off 20 minutes after the last key pressed.

## **Total Suspended Solids (TSS) Instructions**

### **Materials**

1. Filter funnel and manifold
2. 1.5  $\mu\text{m}$ , 47 mm diameter GF/F filters
3. Aluminum pans
4. DI water
5. Balance
6. Tweezers
7. Desiccator

### **Instructions**

#### **Prepping the filters**

1. Place the glass fiber filter on the membrane filter apparatus with wrinkled surface up.
2. While vacuum is applied, wash the disc with three successive 20 mL volumes of DI water. Remove all traces of water by continuing to apply vacuum after water has passed through.
3. Remove filter from membrane filter apparatus and dry in an oven at 103-105°C for one hour.
4. Remove to desiccator and store until needed.
5. Repeat the drying cycle until a constant weight is obtained (weight loss is less than 0.5 mg or less than 4%, whichever is less). Weigh immediately before use. After weighing, handle the filter or crucible/filter with forceps or tongs only.

#### **Filtering and Drying for TSS**

1. Take filters with pan out of the desiccator and bring to the filtration area.
2. With tweezers, place filter on funnel support
3. Snap on funnel, begin suction, and wet the filter with small volume of DI water to seat the filter against the funnel support
4. Agitate sample and use tick marks on funnel to filter at least 100 mL of water

5. With suction on, wash walls of funnel and filter with around 30 mL of DI water
6. Leave suction on for around 3 mins after
7. Carefully remove filter from the filter support with tweezers and place on aluminum pan
8. Dry the filters on the pans for 24 hours in an oven at 103-105°C
9. Cool in desiccator and weigh.

Note: The ideal mass increase for the TSS measurement is between 2 and 200 mg (minimum 1.0 mg). The volume of water sample needed to produce this mass change depends on the TSS value. For water collected under base-flow conditions, the recommended starting volume is 300 mL. However, if the suspended solids collected in the filter are either too high or too low, or if the filtration becomes slow due to clogging (total filtration time > 10 minutes), the volume should be adjusted

# Absorbance Measurement Instructions

## Preparation

- Measuring cup
- 1000 $\mu$ L pipette
- Water samples

## Instructions

1. Open the spectrum machine and computer

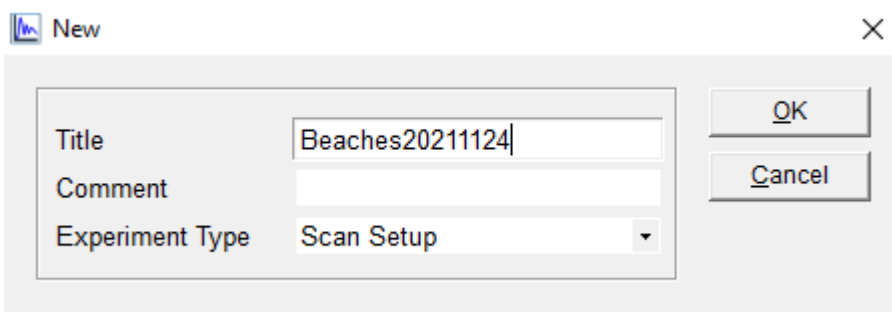
2. Open the UV Express Folder



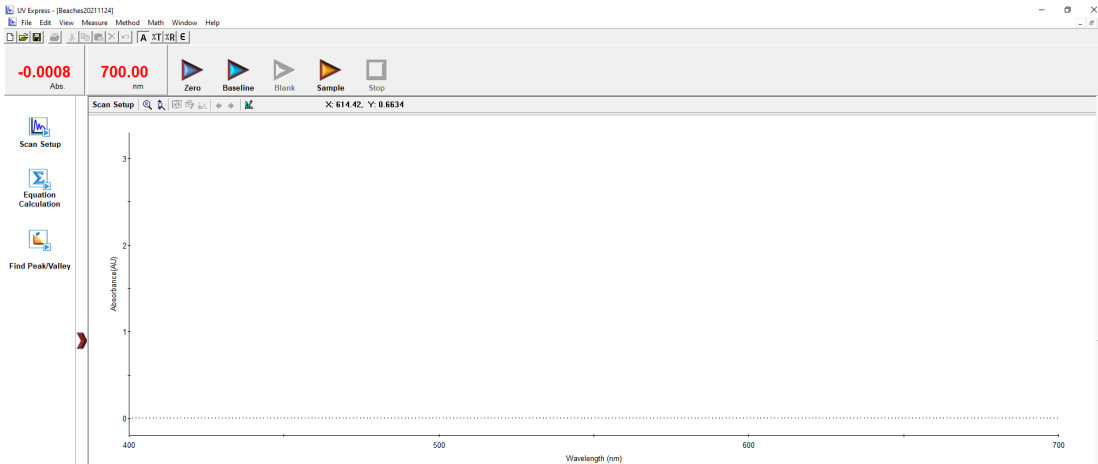
3. Press Scan, and then choose Online

Once the UVExpress shows up, check the cell holder room is empty.

4. Title your file: Beaches + Date

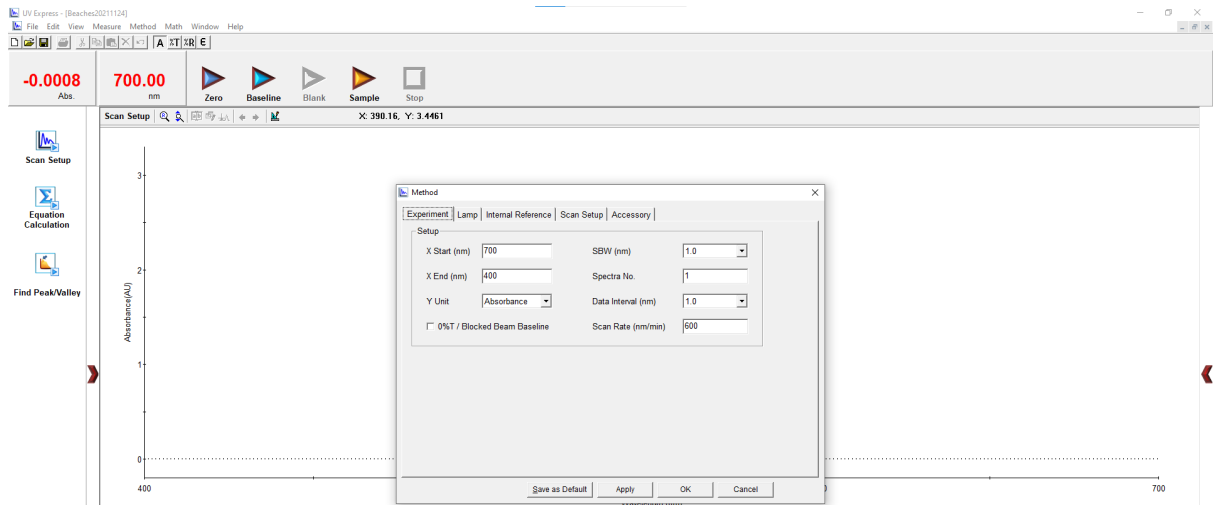


5. Choose Scan setup on the left side.



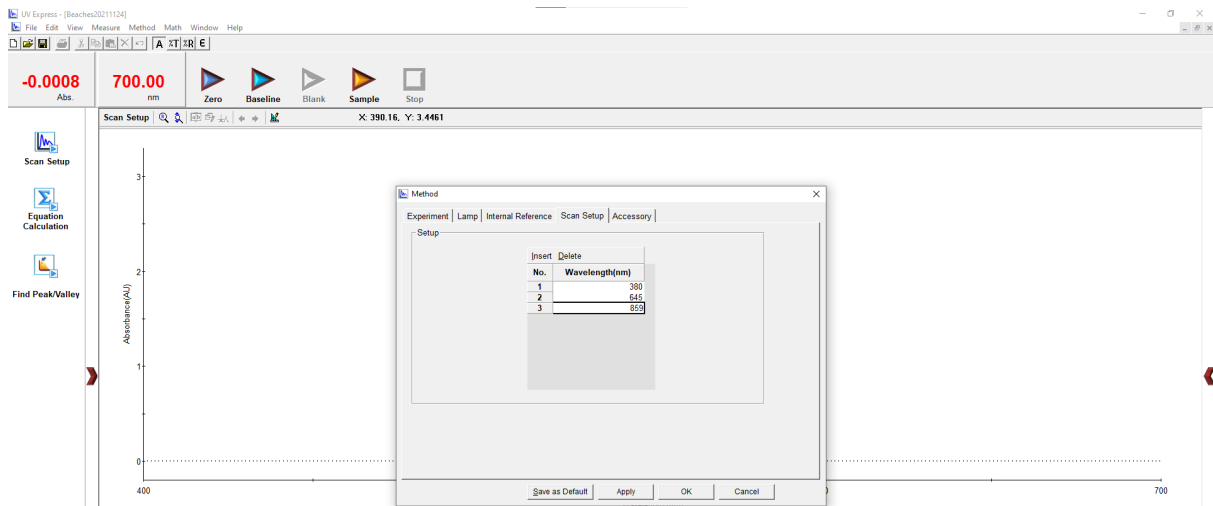
## 6. Choose Experiment

For X start: 1100 nm; X end: 190 nm.



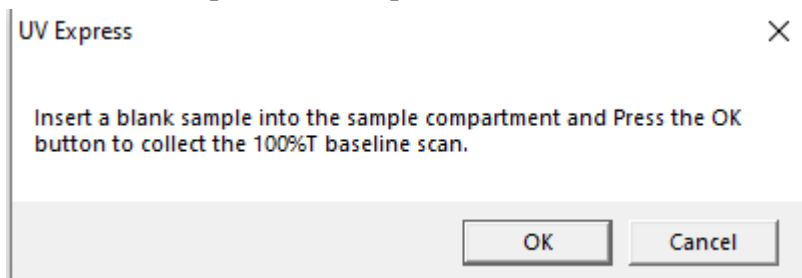
## 7. Choose scan setup

Clear Scan setup, and put in specific wavelength, choose apply.



## 8. Rinse the square cuvettes with MilliQ water.

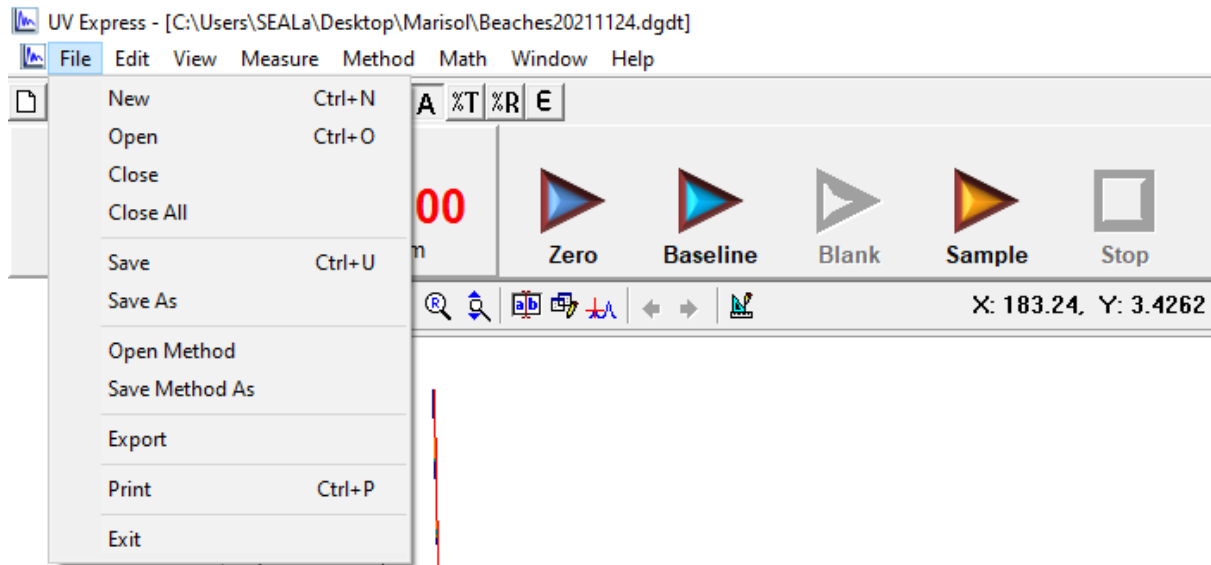
9. Use the pipette to put 1 mL of MilliQ water in both cuvettes, clean the outside of the cuvettes with wipes, and then press baseline.



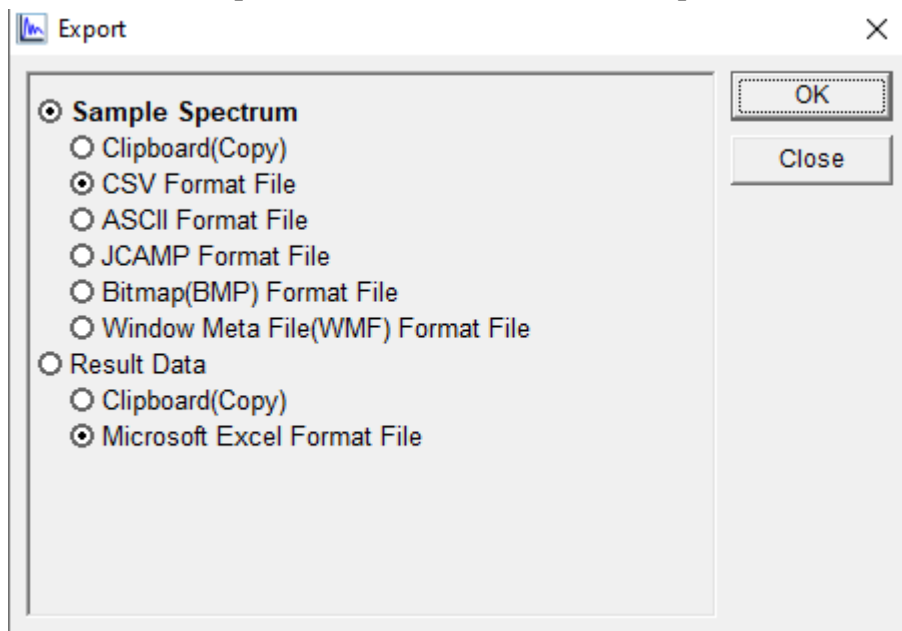
10. After getting the Baseline, take out the sampling cuvette, pour out the MilliQ water and put in sample water instead. Rinse the cuvette with MilliQ water three times if need to test several different samples.

11. Press Sample and name the samples.

12. After testing all the samples, select File - save, save to the desktop.



13. Select File - export, save the cvs file to the desktop for further use.



# Nitrate

DOC316.53.01067

## Cadmium Reduction Method

Method 8192

0.01 to 0.50 mg/L NO<sub>3</sub><sup>-</sup>-N (LR)

Powder Pillows

Scope and application: For water, wastewater and seawater.



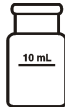
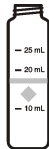
### Test preparation

## Instrument-specific information

Table 1 shows all of the instruments that have the program for this test. The table also shows sample cell and orientation requirements for reagent addition tests, such as powder pillow or bulk reagent tests.

To use the table, select an instrument, then read across to find the applicable information for this test.

**Table 1 Instrument-specific information**

Instrument	Sample cell orientation	Sample cell
DR 6000 DR 3800 DR 2800 DR 2700 DR 1900	The fill line is to the right.	2495402 
DR 5000 DR 3900	The fill line is toward the user.	
DR 900	The orientation mark is toward the user.	2401906 

## Before starting

Install the instrument cap on the DR 900 cell holder before ZERO or READ is pushed.

For the best results, measure the reagent blank value for each new lot of reagent. Replace the sample with deionized water in the test procedure to determine the reagent blank value. Subtract the reagent blank value from the sample results automatically with the reagent blank adjust option.

This method is technique-sensitive. Shaking time and technique influence the color development. For most accurate results, use a standard solution that is within the test range and run the test several times. Increase or decrease the shaking time to get the expected result. Use the adjusted shaking time for sample measurements.

The reagents that are used in this test contain cadmium. Rinse the sample cell immediately after use to remove all cadmium particles. Collect the reacted samples for safe disposal.

A deposit of unoxidized metal will remain at the bottom of the sample cell after the reagent dissolves. The deposit will not affect results.

UV light changes the color of the prepared sample to yellow. Keep the prepared sample out of direct sunlight.

Review the Safety Data Sheets (MSDS/SDS) for the chemicals that are used. Use the recommended personal protective equipment.

Dispose of reacted solutions according to local, state and federal regulations. Refer to the Safety Data Sheets for disposal information for unused reagents. Refer to the environmental, health and safety staff for your facility and/or local regulatory agencies for further disposal information.

## Items to collect

Description	Quantity
NitraVer <sup>®</sup> 6 Nitrate Reagent Powder Pillow, 10-mL	1
NitriVer <sup>®</sup> 3 Nitrite Reagent Powder Pillow, 10-mL	1
Cylinder, graduated mixing, 25-mL	1
Sample cells (For information about sample cells, adapters or light shields, refer to <a href="#">Instrument-specific information</a> on page 1.)	2

Refer to [Consumables and replacement items](#) on page 6 for order information.

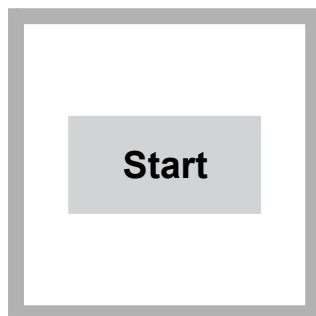
## Sample collection and storage

- Collect samples in clean glass or plastic bottles.
- Analyze the samples as soon as possible for best results.
- If immediate analysis is not possible, immediately filter and keep the samples at or below 6 °C (43 °F) for a maximum of 48 hours.
- To preserve samples for a maximum of 28 days, adjust the sample pH to 2 or less with concentrated sulfuric acid (approximately 2 mL per liter) and keep at or below 6 °C (43 °F). The test results then include nitrate and nitrite.
- Let the sample temperature increase to room temperature before analysis.
- Before analysis, adjust the pH to 7 with 5 N sodium hydroxide solution.
- Correct the test result for the dilution caused by the volume additions.

## Powder pillow procedure

### ⚠ CAUTION

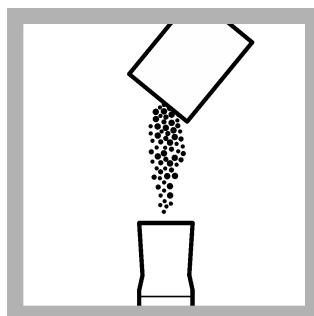
Hazardous waste exposure. Prepared samples contain cadmium. Refer to the SDS for safe handling and disposal instructions. Obey all local and regional disposal regulations.



**1. Start program 351 N, Nitrate LR.** For information about sample cells, adapters or light shields, refer to [Instrument-specific information](#) on page 1.



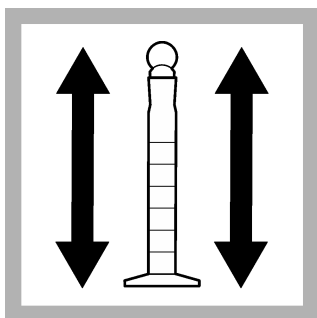
**2. Fill the mixing cylinder with 15 mL of sample.**



**3. Add the contents of one NitraVer 6 Reagent Powder Pillow to the cylinder. Close the cylinder.**



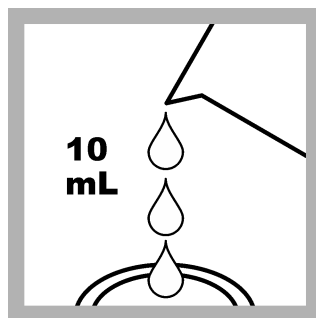
**4. Start the instrument timer. A 3-minute reaction time starts.**



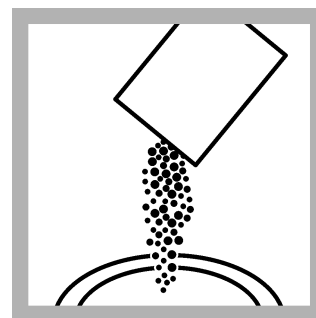
5. Shake the cylinder vigorously during the reaction period. Some powder may not dissolve.



6. When the timer expires, start the timer again. A 2-minute reaction time starts.



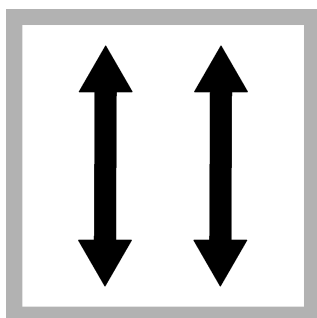
7. **Prepare the sample:** When the timer expires, carefully pour 10 mL of sample into a sample cell. Do not transfer cadmium particles to the sample cell.



8. Add the contents of one NitrVer 3 Reagent Powder Pillow to the prepared sample cell.



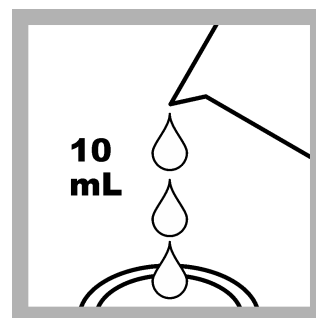
9. Start the instrument timer. A 30-second reaction time starts.



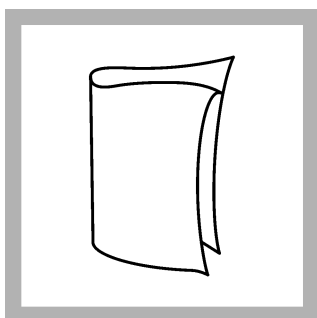
10. Put the stopper on the sample cell. Shake the sample cell gently during the 30-second timer. A pink color shows if nitrate is present in the sample.



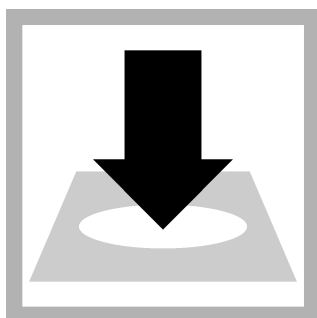
11. Start the instrument timer. A 15-minute reaction time starts.



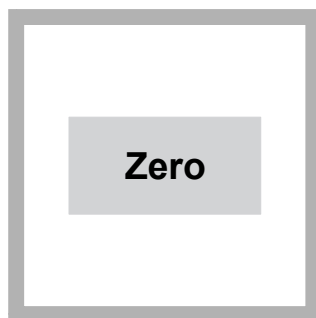
12. **Prepare the blank:** When the timer expires, fill a second sample cell with 10 mL of the original sample.



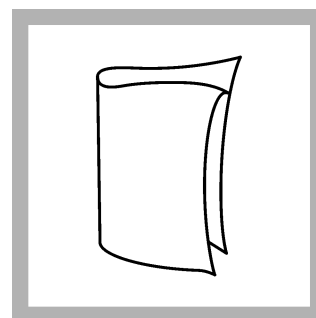
13. Clean the blank sample cell.



14. Insert the blank into the cell holder.



15. Push **ZERO**. The display shows 0.00 mg/L  $\text{NO}_3^-$ -N.



16. Clean the prepared sample cell.



**17.** Insert the prepared sample into the cell holder.



**18.** Push **READ**. Results show in mg/L  $\text{NO}_3^-$ -N.

# Nitrogen, Ammonia

DOC316.53.01077

## Salicylate Method<sup>1</sup>

0.01 to 0.50 mg/L NH<sub>3</sub>-N

Method 8155

Powder Pillows

**Scope and application:** For water, wastewater and seawater.

<sup>1</sup> Adapted from Clin. Chim. Acta., 14, 403 (1966).



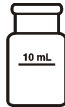
### Test preparation

## Instrument-specific information

Table 1 shows all of the instruments that have the program for this test. The table also shows sample cell and orientation requirements for reagent addition tests, such as powder pillow or bulk reagent tests.

To use the table, select an instrument, then read across to find the applicable information for this test.

**Table 1 Instrument-specific information**

Instrument	Sample cell orientation	Sample cell
DR 6000 DR 3800 DR 2800 DR 2700 DR 1900	The fill line is to the right.	2495402 
DR 5000 DR 3900	The fill line is toward the user.	
DR 900	The orientation mark is toward the user.	2401906 

## Before starting

Install the instrument cap on the DR 900 cell holder before ZERO or READ is pushed.

The reagents that are used in this test contain sodium nitroferricyanide. **Keep cyanide solutions at pH > 11 to prevent exposure to hydrogen cyanide gas.** Collect the reacted samples for safe disposal.

Keep the samples sealed at all times to prevent ammonia contamination from the air.

Review the Safety Data Sheets (MSDS/SDS) for the chemicals that are used. Use the recommended personal protective equipment.

Dispose of reacted solutions according to local, state and federal regulations. Refer to the Safety Data Sheets for disposal information for unused reagents. Refer to the environmental, health and safety staff for your facility and/or local regulatory agencies for further disposal information.

## Items to collect

Description	Quantity
Ammonia Cyanurate Reagent Powder Pillow, 10-mL	2
Ammonia Salicylate Reagent Powder Pillow, 10-mL	2

## Items to collect (continued)

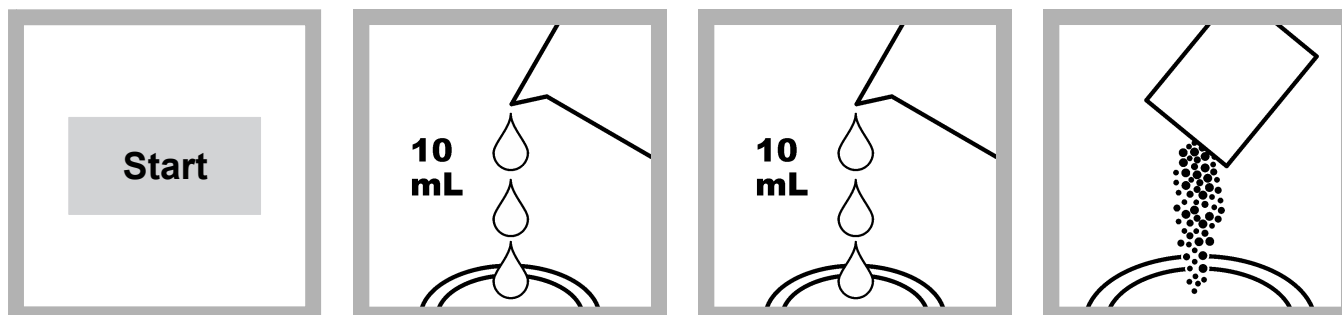
Description	Quantity
Stoppers for 18-mm tubes and AccuVac Ampuls	2
Sample cells (For information about sample cells, adapters or light shields, refer to <a href="#">Instrument-specific information</a> on page 1.)	2

Refer to [Consumables and replacement items](#) on page 5 for order information.

## Sample collection and storage

- Collect samples in clean glass or plastic bottles.
- If the sample contains chlorine, add one drop of 0.1 N sodium thiosulfate to 1 liter of sample to remove each 0.3 mg/L of chlorine.
- To preserve samples for later analysis, adjust the sample pH to less than 2 with concentrated sulfuric acid (approximately 2 mL per liter). No acid addition is necessary if the sample is tested immediately.
- Keep the preserved samples at or below 6 °C (43 °F) for a maximum of 28 days.
- Let the sample temperature increase to room temperature before analysis.
- Before analysis, adjust the pH to 7 with 5 N sodium hydroxide solution.
- Correct the test result for the dilution caused by the volume additions.

## Powder pillow procedure



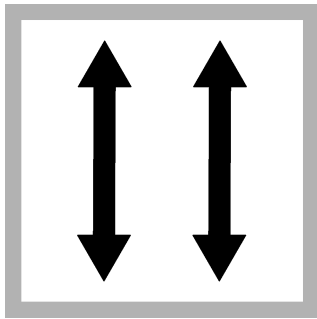
1. Start program **385 N, Ammonia, Salic.** For information about sample cells, adapters or light shields, refer to [Instrument-specific information](#) on page 1.

2. **Prepare the blank:** Fill a sample cell with 10 mL of deionized water.

3. **Prepare the sample:** Fill a second sample cell with 10 mL of sample.

4. Add the contents of one Ammonia Salicylate powder pillow to each sample cell.

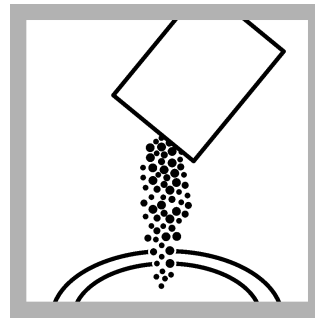
**Note:** Although the program name can be different between instruments, the program number does not change.



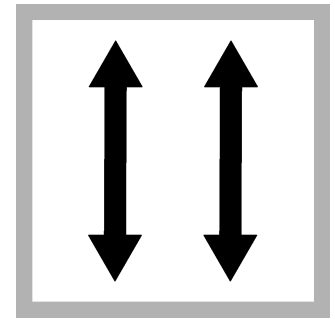
5. Put the stopper on the sample cell. Shake to dissolve the reagent.



6. Start the instrument timer. A 3-minute reaction time starts.



7. After the timer expires, add the contents of one Ammonia Cyanurate powder pillow to each sample cell.

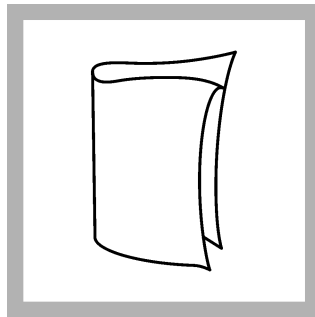


8. Put the stopper on the sample cell. Shake to dissolve the reagent.

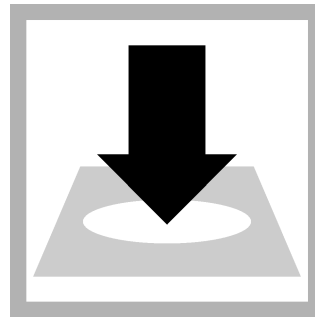


9. Start the instrument timer. A 15-minute reaction time starts.

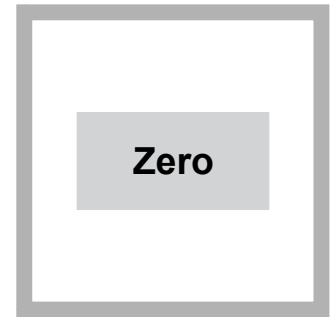
A green color shows when ammonia-nitrogen is present.



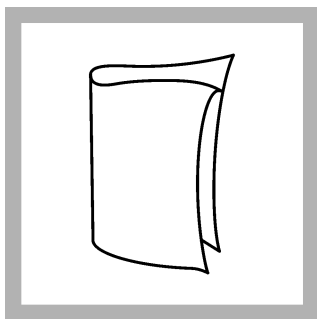
10. When the timer expires, clean the blank sample cell.



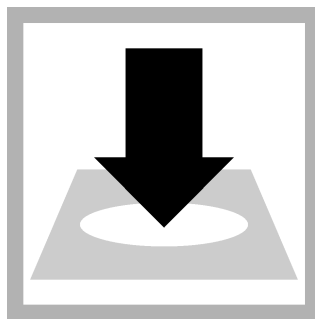
11. Insert the blank into the cell holder.



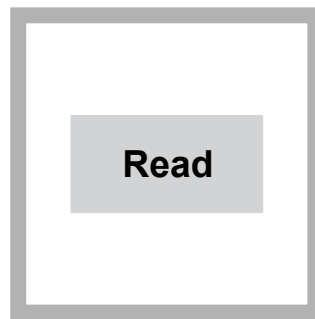
12. Push **ZERO**. The display shows 0.00 mg/L  $\text{NH}_3\text{-N}$ .



13. Clean the prepared sample cell.



14. Insert the prepared sample into the cell holder.



15. Push **READ**. Results show in mg/L  $\text{NH}_3\text{-N}$ .

# Phosphorus, Reactive (Orthophosphate)

USEPA <sup>1, 2</sup> PhosVer<sup>®</sup> 3 Method<sup>3</sup>

Method 8048

0.06 to 5.00 mg/L PO<sub>4</sub><sup>3-</sup> (0.02 to 1.60 mg/L P)

Test 'N Tube™ Vials

**Scope and application:** For drinking water, wastewater and seawater.

<sup>1</sup> USEPA accepted for reporting wastewater analysis. Procedure is equivalent to USEPA and Standard Method 4500-P E for wastewater.

<sup>2</sup> USEPA Accepted for reporting for drinking water analysis. Procedure is an acceptable version of EPA Method 365.1, approved at 40 CFR part 141 NPDWR compliance monitoring.

<sup>3</sup> Adapted from Standard Methods for the Examination of Water and Wastewater.



## Test preparation

### Instrument-specific information

Table 1 shows all of the instruments that have the program for this test. The table also shows adapter and light shield requirements for the instruments that use them.

To use the table, select an instrument, then read across to find the applicable information for this test.

**Table 1 Instrument-specific information for test tubes**

Instrument	Adapters	Light shield
DR 6000, DR 5000	—	—
DR 3900	—	LZV849
DR 3800, DR 2800, DR 2700	—	LZV646
DR 1900	9609900 (D <sup>1</sup> )	—
DR 900	4846400	Cover supplied with the instrument

### Before starting

Install the instrument cap on the DR 900 cell holder before ZERO or READ is pushed.

DR 3900, DR 3800, DR 2800 and DR 2700: Install the light shield in Cell Compartment #2 before this test is started.

For the best results, measure the reagent blank value for each new lot of reagent. Replace the sample with deionized water in the test procedure to determine the reagent blank value. Subtract the reagent blank value from the sample results automatically with the reagent blank adjust option.

Review the Safety Data Sheets (MSDS/SDS) for the chemicals that are used. Use the recommended personal protective equipment.

Dispose of reacted solutions according to local, state and federal regulations. Refer to the Safety Data Sheets for disposal information for unused reagents. Refer to the environmental, health and safety staff for your facility and/or local regulatory agencies for further disposal information.

### Items to collect

Description	Quantity
PhosVer <sup>®</sup> 3 Reagent Powder Pillow	1
Reactive Phosphorus Test 'N Tube Vial	1
Funnel, micro	1

<sup>1</sup> The D adapter is not available with all instrument versions.

## Items to collect (continued)

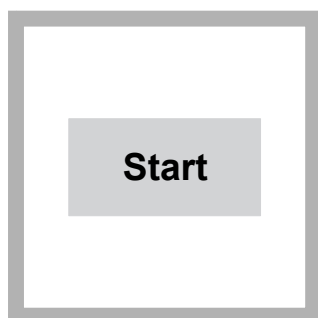
Description	Quantity
Light shield or adapter (For information about sample cells, adapters or light shields, refer to <a href="#">Instrument-specific information</a> on page 1.)	1
Pipet, TenSette <sup>®</sup> , 1.0- to 10.0-mL, with pipet tips	1
Test tube rack	1

Refer to [Consumables and replacement items](#) on page 4 for order information.

## Sample collection and storage

- Collect samples in clean glass or plastic bottles that have been cleaned with 6 N (1:1) hydrochloric acid and rinsed with deionized water.
- Do not use a detergent that contains phosphate to clean the sample bottles. The phosphate in the detergent will contaminate the sample.
- Analyze the samples as soon as possible for best results.
- If immediate analysis is not possible, immediately filter and keep the samples at or below 6 °C (43 °F) for a maximum of 48 hours.
- Let the sample temperature increase to room temperature before analysis.

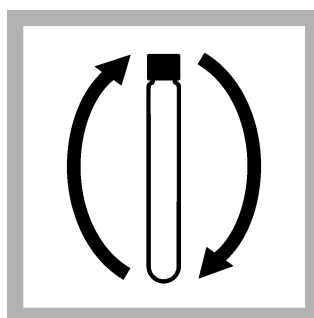
## Test 'N Tube procedure



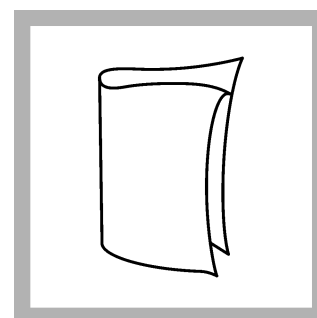
1. Start program **535 P React. PV TNT**. For information about sample cells, adapters or light shields, refer to [Instrument-specific information](#) on page 1.



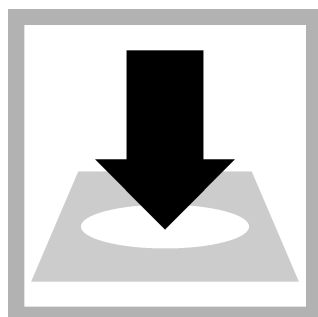
2. Add 5.0 mL of sample to a Reactive Phosphorus Test 'N Tube Vial.



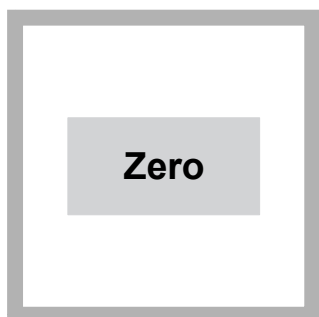
3. Put the cap on the vial. Invert to mix.



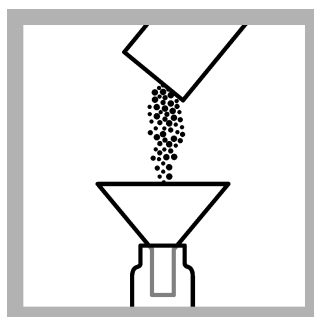
4. Clean the vial.



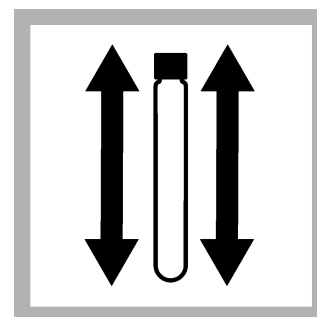
5. Insert the vial into the 16-mm cell holder.



6. Push **ZERO**. The display shows 0.00 mg/L  $\text{PO}_4^{3-}$ .



7. Add the contents of one PhosVer 3 Phosphate Powder Pillow.

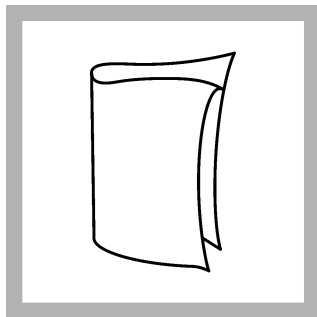


8. Put the cap on the vial. Shake for at least 20 seconds. The powder will not dissolve completely.

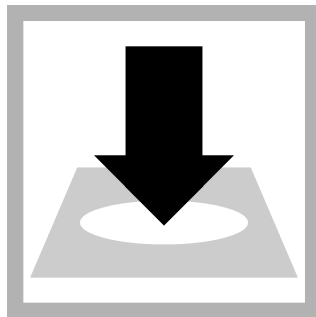


**9.** Start the instrument timer. A 2-minute reaction time starts.

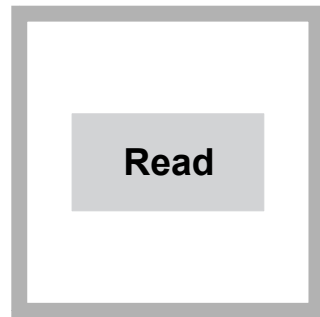
Measure the sample between two and eight minutes after adding the PhosVer 3 reagent.



**10.** When the timer expires, clean the vial.



**11.** Insert the vial into the 16-mm cell holder.



**12.** Push **READ**. Results show in mg/L  $\text{PO}_4^{3-}$ .

## Water FIB SOP

### Preparation

1. Clear Marisol's bench and wipe with ethanol
2. Gather supplies
  - a. Nalgene bottles (2 per site)
  - b. Graduated cylinder
  - c. 5,000 uL pipette
  - d. 5,000 uL pipette tips (1 per site)
  - e. IDEXX Quanti-Tray (2 per site)
  - f. IDEXX Colilert powder packets (1 per site)
  - g. IDEXX Enterolert powder packets (1 per site)
  - h. Metal baskets
  - i. MiliQ Water bottles
  - j. Samples
3. Turn on the Quanti-Tray Sealer (Red-On and Green-Ready)

### Procedure

1. Label Nalgene bottles and IDEXX Quanti-Trays (Site-Date-Test-Dilution)
2. Add 90 mL of MiliQ Water into all the bottles
3. Add the IDEXX Colilert powder packet to half of the bottles
4. Add the IDEXX Enterolert powder packet to the other half of the bottles
5. Shake bottles until the reagents dissolve
6. Shake sample bottle and add 10 mL (5,000 uL x2) of sample into one Colilert bottle and into one Enterolert bottle
7. Repeat step 6 for each site
8. Pour the contents of each Nalgene bottle into the designated Quanti-Tray and keep upright using a metal basket
9. Carefully place a Quanti-Tray into the Quanti-Tray rubber insert
10. Insert the Quanti-Tray rubber insert into the Quanti-Tray Sealer
11. Repeat steps 9-10 for each site
12. Incubate Colilert trays laid flat with seal up at  $35^{\circ}\text{C} \pm 0.5^{\circ}\text{C}$  for 18 - 22 hours
13. Incubate Enterolert trays laid flat with seal up at  $41^{\circ}\text{C} \pm 0.5^{\circ}\text{C}$  for 24 hours
14. Record the time when you began incubating
15. Turn off the Quanti-Tray Sealer and clean up

### Colilert Counts

1. Clear the extraction station and wipe down with ethanol
2. Take a Quanti-Tray, draw a dash on all the yellow squares, and record total coliforms  
(TC:  $\frac{\text{Yellow Big Squares}}{\text{Yellow Small Squares}}$ )
3. Repeat step 2 for each site
4. Turn UV box on

5. Insert a Quanti-Tray into the UV box, draw a perpendicular dash on all the fluorescent squares, and record *Escherichia coli* (EC:  $\frac{\text{Fluorescent Big Squares}}{\text{Fluorescent Small Squares}}$ )
6. Repeat step 5 for each site
7. Record data
8. Leave trays on Marisol's bench, turn off UV box, and clean up

#### Enterolert Counts

1. Clear the extraction station and wipe down with ethanol
2. Turn UV box on
3. Insert a Quanti-Tray into the UV box, draw a dash on all the fluorescent squares, and record enterococci (ENT:  $\frac{\text{Fluorescent Big Squares}}{\text{Fluorescent Small Squares}}$ )
4. Record data
5. Leave trays on Marisol's bench, turn off UV box, and clean up

For more information and a video of the procedures visit:

[www.idexx.com/en/water/water-products-services/colilert-18/](http://www.idexx.com/en/water/water-products-services/colilert-18/)

<https://www.idexx.com/en/water/water-products-services/enterolert/>

## ARB Membrane Filtration SOP

### Preparation

1. Clear the filtration station and wipe with ethanol
2. Gather supplies
  - a. Funnels (1 per site + 1 for blanks)
  - b. Filters (0.2 and 0.45  $\mu\text{m}$ )
  - c. Tweezers
  - d. Ethanol jar (away from Bunsen burner)
  - e. 5 mL syringe
  - f. PBS bottles
  - g. Samples
  - h. +/- mTEC plates (2 (+) (antibiotic present) and 2 (-) (no antibiotic) per site)
3. Check that the Bunsen burner is connected to the gas spout. Turn the gas valve halfway and use the spark lighter to light the Bunsen burner. Lower the gas valve until you see a blue flame
4. Check that the manifold filtration system is connected to the vacuum spout. Turn the vacuum valve all the way
5. Place funnels onto the bases of the manifold filtration system

### Filtering Sample for the Plate Method

1. Sterilize tweezers (dip them in the ethanol jar and hold them in the flame for a few seconds)
2. Remove the top of a funnel
3. Use sterile tweezers to remove and discard the gridded filter from the funnel cotton pad
4. Use sterile tweezers to place the 0.45  $\mu\text{m}$  membrane (with grid side up) onto the funnel cotton pad and then place a 20  $\mu\text{m}$  filter on top.
5. Snap on the top of the funnel
6. filter your sample water to a countable dilution volume (turn the valve from the manifold filtration system all the way)
7. Filter 5-10 mL of PBS through the membrane and filter to rinse the filter cup.
7. Carefully remove the top of the funnel
8. Use sterile tweezers to discard the 20  $\mu\text{m}$  filter
9. Place 0.45  $\mu\text{m}$  membrane on the mTEC agar plate with grid side up and no space or air bubbles between filter and agar.
10. Incubate plates at  $44.5^{\circ}\text{C} \pm 0.2^{\circ}\text{C}$  for  $22 \pm 2$  hours.
11. Count and record colonies for both + and - plates.

### Volume for filtration per beach site:

Venice Beach ~ 500ml (for (+) plates) and 500 ml (for (-) plates)

Santa Monica ~ 700ml (for (+) plates) and 10 ml (for (-) plates)

Malibu 1 ~ 500ml (for (+/-) plates)

Malibu 2 ~ 850ml (for (+) plates) and 150 ml (for (-) plates)

Malibu 3 ~ 900ml (for (+) plates) and 100 ml (for (-) plates)

Palisades ~ 500ml (for (+) plates) and 500 ml (for (-) plates)

Zuma ~ 500ml (for (+) plates) and 500 ml (for (-) plates)

Topanga ~ 500ml (for (+) plates) and 500 ml (for (-) plates)

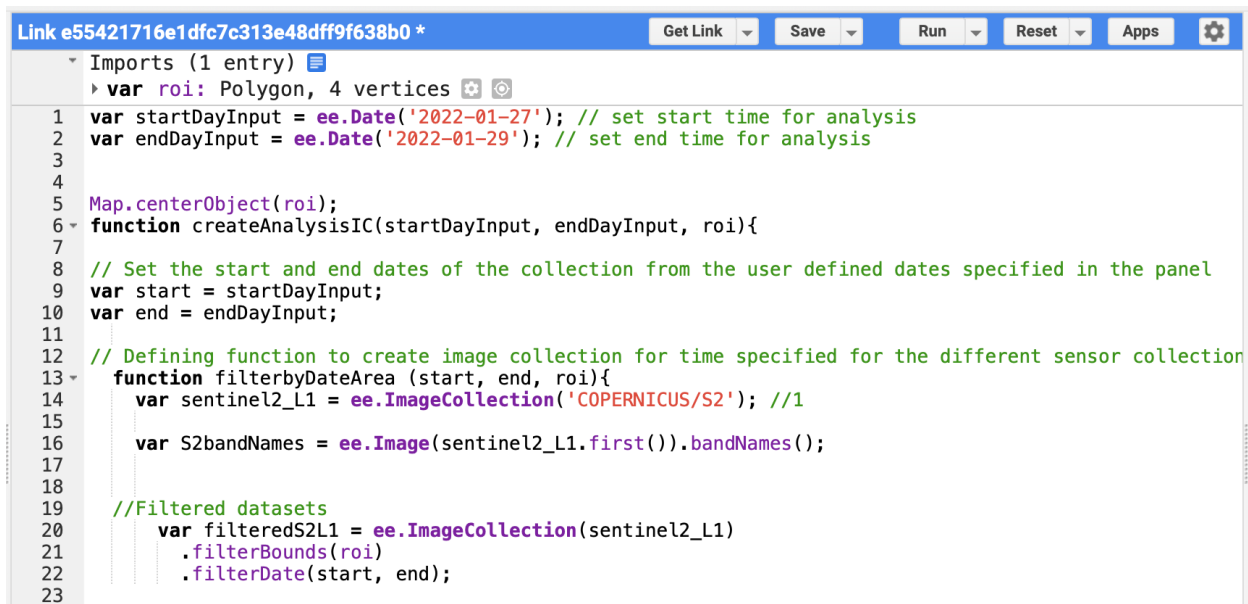
1. **Install Python 3.7 (check “Add Python 3.7 to PATH”):**  
<https://www.python.org/downloads/>
2. **Install Anaconda (leave all defaults as is):**  
<https://www.anaconda.com/products/individual>
3. **Install libraries for ACOLITE in Anaconda Prompt**
  - a. **Open Anaconda Prompt**
  - b. **Create environment (copy and paste)**  
conda create --name ACOLITE
  - c. **Install ACOLITE dependencies (copy and paste one line at a time)**  
conda activate ACOLITE  
conda install -n ACOLITE netcdf4  
conda install -c conda-forge/label/cf202003 gdal -n ACOLITE  
conda install -c conda-forge matplotlib -n ACOLITE  
conda install -c conda-forge numpy -n ACOLITE  
conda install -c anaconda scipy -n ACOLITE  
conda install -c conda-forge requests -n ACOLITE  
conda install -c conda-forge pillow -n ACOLITE  
conda install -c conda-forge pyproj -n ACOLITE  
conda install -c conda-forge statsmodels -n ACOLITE  
conda install -c conda-forge pyhdf -n ACOLITE  
conda install -c conda-forge rasterio -n ACOLITE  
conda install -c conda-forge scikit-image -n ACOLITE  
conda install -c conda-forge pyresample -n ACOLITE
4. **Install ACOLITE**
  - a. **Create a new folder on your desktop and name it ACOLITE**
  - b. **Download ACOLITE:** <https://github.com/acolite/acolite>
  - c. **Extract the file and move it to the ACOLITE folder on your desktop**
  - d. **Go to** acolite-master>config>acolite\_defaults.txt
  - e. **Open** acolite\_defaults.txt **and under # GeoTIFF export options modify False to True**  
l2r\_export\_geotiff=True  
l2w\_export\_geotiff=True
5. **Download imagery**
  - a. **Create two new folders in the ACOLITE folder and name one Input and the other Output**
  - b. **Create a USGS account:** <https://earthexplorer.usgs.gov/>
  - c. **Under Search Criteria pin a location or insert coordinates**
  - d. **Under Date Range select dates of interest**
  - e. **Under Cloud Cover specify 0-60%**
  - f. **Click Data Sets and select Sentinel-2 or Landsat 8-9 OLI/TIRS C2 L1**
  - g. **Click Results**
  - h. **Click Download Options (icon with green downward arrow)**
  - i. **Download L1C Tile in JPEG2000 format for Sentinel-2 images and** (click on product options) **Level-1 GeoTIFF Data Product for Landsat 8-9 OLI/TIRS C2 L1 (takes a while to download)**
  - j. **Extract the file and move it to the Input folder**
6. **Process imagery in Anaconda prompt:**
  - a. **Open Anaconda Prompt**

- b. Activate environment**  
conda activate ACOLITE
- c. Set directory to ACOLITE folder (insert your path, this is my path as an example)**
- d.** cd C:\Users\Desktop\ACOLITE\acolite-master
- e. Launch ACOLITE**  
python launch\_acolite.py
- f. In ACOLITE GUI**
  - i.** Under Input **select file in Input folder**
  - ii.** Under Output **select Output folder (before you run an image ensure this folder is clear)**
  - iii.** Under Region of Interest **input coordinates**
    - 1. South: 33.7181, North: 34.1323, West: -118.9551, East: -118.2191
  - iv.** Under **L2W parameters type tur\_dogliotti2015**
  - v.** **Check L2W parameters**
  - vi.** **Click Run Processing**
  - vii.** **Open the Output folder and move the image ending in t\_dogliotti.tif to a folder where you will save your processed images. You can delete the rest of the files in the Output folder**

## Appendix J: Google Earth Engine

Link to public GEE script:

<https://code.earthengine.google.com/ae9ac5998269affaa14d938e42429fe9>



```
Link e55421716e1dfc7c313e48dff9f638b0 *  Get Link  Save  Run  Reset  Apps  ⚙️
Imports (1 entry)
  var roi: Polygon, 4 vertices
1 var startDayInput = ee.Date('2022-01-27'); // set start time for analysis
2 var endDayInput = ee.Date('2022-01-29'); // set end time for analysis
3
4
5 Map.centerObject(roi);
6 function createAnalysisIC(startDayInput, endDayInput, roi){
7
8 // Set the start and end dates of the collection from the user defined dates specified in the panel
9 var start = startDayInput;
10 var end = endDayInput;
11
12 // Defining function to create image collection for time specified for the different sensor collection
13 function filterbyDateArea (start, end, roi){
14   var sentinel2_L1 = ee.ImageCollection('COPERNICUS/S2'); //1
15
16   var S2bandNames = ee.Image(sentinel2_L1.first()).bandNames();
17
18
19 //Filtered datasets
20   var filteredS2L1 = ee.ImageCollection(sentinel2_L1)
21     .filterBounds(roi)
22     .filterDate(start, end);
23
```